CHARACTERIZATION AND PROPERTIES OF AMORPHOUS Si:N AND Si:N:H ALLOYS

GORO SASAKI

DECEMBER 1983

DEPARTMENT OF ELECTRICAL ENGINEERING
KYOTO UNIVERSITY
KYOTO, JAPAN

CHARACTERIZATION AND PROPERTIES OF AMORPHOUS Si:N AND Si:N:H ALLOYS

GORO SASAKI

DECEMBER 1983

DEPARTMENT OF ELECTRICAL ENGINEERING
KYOTO UNIVERSITY
KYOTO, JAPAN

DOC
1983
5
電気系

The works of the author during his doctor course from April 1981 to December 1983 in Department of Electrical Engineering, Kyoto University, are described. This book is submitted to Faculty of Engineering, Kyoto University, for his doctor dissertation.

ABSTRACT

Characterization and properties of amorphous silicon-nitrogen (a-Si:N) alloys deposited by chemical vapor deposition (CVD) and amorphous silicon-nitrogen-hydrogen (a-Si:N:H) alloys by glow-discharge (GD) deposition are investigated and described.

A new method and improved method on measurements of the gap-state density of CVD a-Si are proposed and demonstrated. The gap-state density of CVD a-Si films deposited at 550°C from SiH_4 in Ar gas is evaluated by these methods. Response time, capture cross section, and density of traps in metal/insulator/semiconductor structures where the semiconductor is CVD a-Si:N or GD a-Si:H alloys are evaluated from the frequency and temperature dependence of the flat-band capacitance.

Amorphous Si:N alloys are prepared by chemical vapor deposition of SiH_4, NH_3, and Ar gases at 550°C. The deposition rate and nitrogen content of films at various SiH_4 and NH_3 gas concentrations are measured, and the deposition process of films and the nitrogen incorporation process into films are discussed.

Optical and electrical properties of CVD a-Si:N films are described, and influences of the nitrogen incorporation on their properties, defects, and gap states are investigated. The nitrogen incorporation widens the optical gap, decreases the refractive index, and eliminates the hopping conduction around room temperature. The paramagnetic defects detected by electron spin resonance and gap-state density evaluated by the field-effect method are decreased by the nitrogen incorporation.

Thermal annealing of CVD a-Si:N films increases the hopping conduction, the number of paramagnetic defects, the gap-state density evaluated by the field-effect method. Post-hydrogenation of CVD a-Si:N films increases the dark conductivity and photo-response.

Amorphous Si:N:H alloys are prepared by glow-discharge decompo-

sition of SiH_4, N_2, and H_2 gases. The dependence of nitrogen and hydrogen contents in films on deposition conditions is described. Optical and electrical properties of films are described, and their dependence on deposition conditions is investigated.

ACKNOWLEDGMENTS

I would like to express my deep gratitude to *Professor Akio Sasaki* for his favorable support and advices throughout this work. I am grateful to *Professors Akira Kawabata and Hiroyuki Matsunami* for their useful comments on the manuscript. I am very indebted to *Mr. Shizuo Fujita, Dr. Yoshikazu Takeda, and Dr. Shigeo Fujita* for their advices in experiments and discussions.

I would like to acknowledge *Dr. Takashi Kawamura, Department of Hydrocarbon Chemistry, Kyoto University*, for his assistance in the ESR measurements. Experiments in this study were also partly supported by facilities of *Matsunami Laboratory, Takagi Laboratoty*, and *Kawabata Laboratory*, and collaborative works of *Messrs. Masayuki Fujita, Makoto Kondo, Toshiyuki Tanaka, Masaya Okamoto*, and *Hideo Toyoshima*.

CONTENTS

I. INTRODUCTION 1

References 3

II. CHARACTERIZATION OF GAP STATES IN AMORPHOUS SILICON 5

2.1 Introduction 5
2.2 High-Frequency Capacitance-Voltage Method 7
2.3 Field-Effect Method for CVD a-Si 9
2.4 Results on Gap-State Density of CVD a-Si 13
2.5 MIS Capacitance-Frequency-Temperature Measurement 13
2.6 Summary 16

References 17

III. CHEMICAL VAPOR DEPOSITION OF AMORPHOUS SILICON-NITROGEN ALLOYS 19

3.1 Introduction 19
3.2 Preparation 19
3.3 Deposition Rate 21
3.4 Infrared Absorption and Nitrogen Content 24
3.5 Summary 27

References 28

IV. OPTICAL PROPERTIES OF CHEMICALLY VAPOR-DEPOSITED AMORPHOUS SILICON-NITROGEN ALLOYS 31

4.1 Introduction 31
4.2 Experiments 32
4.3 Optical Absorption and Optical Gap 34
4.4 Refractive Index 37
4.5 Summary 37

References 38

V. ELECTRICAL PROPERTIES OF CHEMICALLY VAPOR-DEPOSITED AMORPHOUS SILICON-NITROGEN ALLOYS 39

5.1 Introduction 39
5.2 Dark Conductivity 39
5.3 Photoresponse 43
5.4 Summary 45

References 45

VI. DEFECTS AND GAP STATES IN CHEMICALLY VAPOR-DEPOSITED AMORPHOUS SILICON-NITROGEN ALLOYS 47

6.1 Introduction 47
6.2 Electron Spin Resonance (ESR) 47
6.3 Gap-State Density Evaluated by Field-Effect Method 49
6.4 Summary 52

References 53

VII. THERMAL ANNEALING OF CHEMICALLY VAPOR-DEPOSITED AMORPHOUS SILICON-NITROGEN ALLOYS 55

7.1 Introduction 55
7.2 Thermal Annealing 56
7.3 Electron Spin Resonance (ESR) 56
7.4 Dark Conductivity 57
7.5 Gap-State Density Evaluated by Field-Effect Method 59
7.6 Summary 60

References 61

VIII. POST-HYDROGENATION OF CHEMICALLY VAPOR-DEPOSITED AMORPHOUS SILICON-NITROGEN ALLOYS 63

8.1 Introduction 63
8.2 Post-Hydrogenation 63
8.3 Dark Conductivity 64
8.4 Photoconductivity — Product of Quantum Efficiency, Mobility, and Lifetime 67
8.5 Summary 67

References 68

IX. GLOW-DISCHARGE DEPOSITION OF AMORPHOUS SILICON-NITROGEN-HYDROGEN ALLOYS 71

9.1 Introduction 71
9.2 Preparation 71
9.3 Deposition Rate 72
9.4 Infrared Absorption — Nitrogen and Hydrogen Contents 73
9.5 Summary 75

References 76

X. OPTICAL AND ELECTRICAL PROPERTIES OF GLOW-DISCHARGE DEPOSITED AMORPHOUS SILICON-NITROGEN-HYDROGEN ALLOYS 79

10.1 Introduction 79
10.2 Optical Gap 79
10.3 Dark Conductivity 80

10.4 Photoconductivity — Product of Quantum Efficiency, Mobility, and Lifetime 82
10.5 Summary 83
References 83

XI. CONCLUSIONS 85

APPENDIX 89

A. Energy Band Diagram of Amorphous Si/Crystalline Si Junctions 89
B. Detailed Description on Frequency and Temperature Dependence of a-Si MIS Diode Flat-Band Capacitance 93
C. Derivation of Equation (3.6) 95
D. Derivation of Equation (3.9) 95

ADDENDUM 97
Publications 97
Oral Presentations 98

I. INTRODUCTION

Amorphous silicon-hydrogen (a-Si:H) alloy films are a unique electrical material. These films can be grown onto various substrates without loosing their applicability to electrical devices. Especially, their effective absorption of solar energy in thin film structure, which results from the high absorption coefficient, makes it possible to fabricate low-cost solar cells onto low-cost substrates.[1,2] Further, various devices can be fabricated by utilizing a-Si:H films, *e.g.*, thin film transistors for large-area liquid-crystal displays,[3] vidicon targets,[4,5] photoconductive drums for xerography or laser printer,[6,7] or photoconductive sensor arrays.[8]

One of important features of semiconductor is the bipolarity of carriers. Most of semiconductor electrical devices are operated due to electrons and holes moving through the conduction band and the valence band, respectively. On the other hand, carriers can be transported via localized states by hopping conduction in amorphous semiconductors.[9] It is supposed that the localized states in amorphous Si originate from structural disorder, *i.e.*, fluctuations in a tetrahedral bond angle and bond length, or breaking the covalent bond. Although the a-Si films in which the hopping conduction dominates are poor for their applications, their applicability can be improved by the hydrogenation.

It is generally understood that electronic states form energy bands even in amorphous semiconductors. It is considered that these bands result from interactions of bonding states, anti-bonding states, or lone-pairs between themselves. The electronic states in a-Si are composed of the conduction band and the valence band resulting from interacting anti-bonding states and bonding states of covalent bonds between Si atoms, respectively, and the defect states. It could be considered that the randomness in atomic configurations introduces the localized states into the conduction band and the valence band, which are often called as the tail states. It is believed that the

band states can be separated by a specific energy, *i.e.*, the mobility edge, into the localized states and the extended states. In other words, it is considered that the localized states are composed of the tail states and defect states, and the localized states are often called by the gap states. Recent innumerable investigations on properties of a-Si:H alloys have shown that the hydrogenation of a-Si films drastically decreases the gap states.

Electrical properties of a-Si and its alloys are strongly influenced by the gap states. It can be considered that the gap states act as (i) trapping centers for mobile carriers in the extended states, (ii) recombination centers of excess carriers, (iii) charged centers which shield applied electric fields, and (iv) compensation centers for active doping of donors or acceptors. The reduction of the gap states is essential to application of a-Si and its alloys to electrical devices.

Since an a-Si:H alloy is a promising photoconductive material, the control of their optical absorption is essential to their wider applications. Although a-Si:H sub-micron-order thin films are semitransparent for visible lights, a-SiN is known to be transparent for them. Thus, a-Si:N:H alloys are interested as a wide optical gap material.[10,11]

In this study, effects of nitrogen incorporation into a-Si and a-Si:H films on their optical and electrical properties are investigated. Although electrical properties are strongly influenced by the gap states, characterization method of the gap states has not yet been established. In Chapter II, reported methods on the gap-state density are reviewed and discussed. A new measurement method and improved method of the gap-state density in a-Si or its alloys are proposed, and their results are presented. Further, a new measurement method of the response time at charging and discharging of traps in metal/insulator/a-Si structure is proposed. In Chapter III, preparation of a-Si:N films by chemical vapor deposition (CVD) is described. Their optical and electrical properties are described in

Chapter IV and V, and influences of the nitrogen incorporation on their properties are discussed. Effects of the nitrogen incorporation on defects and the gap-state density of CVD a-Si are presented and discussed in Chapter VI. Although these CVD a-Si:N films contain little hydrogen atoms, a small amount of incorporated hydrogen atoms could influence their electrical properties. In Chapter VII and VIII, influences of incorporated hydrogen atoms on their properties are investigated in terms of thermal annealing or post-hydrogenation. Preparation of ternary a-Si:N:H alloy films by glow-discharge deposition is described in Chapter IX. Their optical and electrical properties are presented and discussed in Chapter X. The results investigated in this study are summarized in Chapter XI.

REFERENCES

1) D.E. Carlson and C.R. Wronski, Appl. Phys. Lett., 28 (1976) 761.
2) Y. Hamakawa, Solar Energy Materials, 8 (1982) 101.
3) P.G. LeComber, W.E. Spear, and A. Ghaith, Electron. Lett., 15 (1979) 179.
4) I. Shimizu, T. Komatsu, K. Saito, and E. Inoue, J. Non-Cryst. Solids, 35-36 (1980) 773.
5) Y. Imamura, S. Ataka, Y. Takasaki, C. Kurano, T. Hirai, and E. Maruyama, Appl. Phys. Lett., 35 (1979) 349.
6) N. Yamamoto, Y. Nakayama, K. Wakita, M. Nakano, and T. Kawamura, Jpn. J. Appl. Phys., 20 (1981) suppl. 20-1, 305.
7) M. Matsumura, H. Hayama, Y. Nara, and K. Ishibashi, Jpn. J. Appl. Phys., 20 (1981) suppl. 20-1, 311.
8) T. Kagawa, N. Matsumoto, and K. Kumabe, Jpn. J. Appl. Phys., 21 (1982) suppl. 21-1, 311.
9) N.F. Mott and E.A. Davis, *Electronic Processes in Non-Crystalline Materials* (Clarendon, Oxford, 1979), chapter 2.
10) D.A. Anderson and W.E. Spear, Philos. Mag., 35 (1977) 1.
11) H. Kurata, M. Hirose, and Y. Osaka, Jpn. J. Appl. Phys., 20 (1981) L811.

II. CHARACTERIZATION OF GAP STATES IN AMORPHOUS SILICON

2.1 INTRODUCTION

Various measurement techniques for determinig the gap-state density of amorphous silicon (a-Si) or its alloys have been reported.[1-13] They are summarized in Table 2.1 and briefly reviewed.

Methods (i) and (iii) involve the assumption about the magnitude of the parameters, and only the gap-state density around the Fermi level can be evaluated. In method (ii), (iv), and (v), the metal/insulator/a-Si structure is used. In this structure, interface states always exist at the insulator/a-Si interface. Thus, the results may be influenced by these interface states. It is difficult to measure separately the bulk gap-state density from the interface-state density. However, it is possible to estimate the bulk gap-state density, because the influence of the interface-state density on the measurement result can be excluded by using the field-effect method and the low-frequency *C-V* method.[14] In method (iv),

TABLE 2.1 Measurement techniques for determining gap-state density of amorphous Si or its alloys.

	METHOD	STRUCTURE	REFERENCE
(i)	MOTT'S VARIABLE RANGE HOPPING	BULK	1
(ii)	FIELD EFFECT	MIS	2-5
(iii)	AC CONDUCTIVITY	MIS TUNNEL JUNCTION	6
(iv)	CONDUCTANCE	MIS TUNNEL JUNCTION	7
(v)	LOW-FREQUENCY *C-V*	MIS	8
(vi)	DLTS	SCHOTTKY	9
(vii)	ICTS	SCHOTTKY	10
(viii)	FREQUENCY DEPENDENT CAPACITANCE AND CONDUCTANCE	SCHOTTKY	11,12
(ix)	SPACE-CHARGE-LIMITTED CURRENT	BULK	13

the bulk gap-state density has been assumed to equal the 3/2 power of the interface-state density. However, the effective interface-state density is considered to equal the product of the bulk gap-state density and the maximum tunneling distance. Methods (vi) and (vii) can eliminate the influence of interface states and can determine the gap-state density under the appropriate measurement conditions, *i.e.*, the differential capacitance must be measured at a sufficient lower frequency than the inverse of bulk dielectric relaxation time. This requirement limits the measurable energy range. Moreover, the measurements must be carried out at a temperature at which conduction in extended states dominates, since the analysis assumes that the electrons injected into gap states are emitted into extended states within a specific relaxation time after removal of the injection pulses and are then swept out into the bulk. At the low temperatures at which hopping conduction dominates, the electrons injected into gap states are emitted into other gap states and are swept out by hopping conduction. Method (viii) can be used to evaluate the effective gap-state density around the Fermi level by four different ways, *i.e.*, from results of capacitance and conductance measurements in the low-frequency and the high-frequency ranges. The results will be reliable, provided the gap-state density does not vary drastically near the Fermi level. In method (ix), information on the bulk gap-state density can be obtained, provided the energetic distribution of the gap-state density is constant or logarithmic and the carriers are transported by the extended state conduction.

The applicability of these methods to chemically vapor-deposited (CVD) a-Si is discussed. In metal/CVD a-Si junctions, electrons can be tunneled through the junction via gap states, since CVD a-Si contains many gap states. Thus, metal/CVD a-Si junctions do not show rectifying behavior, and the differential capacitance of the junction is hard to be measured. Besides, carrier transport in CVD a-Si is dominated by hopping conduction up to about 150°C. Therefore, methods (vi), (vii), (viii), and (ix) are not applicable to CVD a-Si.

Assumptions about the magnitude of parameters are not desirable, since these values are very difficult to verify. Consequently, it can be considered that only the field-effect method and the MIS low-frequency *C-V* method are suitable for gap-state measurements of CVD a-Si.

In this chapter, measurement of the gap-state density in CVD a-Si by the field-effect method is described. However, the gap-state density at $|E - E_F| \leqq 0.1$ eV cannot be measured precisely by this method. Thus, the high-frequency *C-V* method using a-Si/crystalline Si junctions is proposed and demonstrated as an appropriate measurement technique for the gap-state density around the Fermi level in CVD a-Si.[15] Further, response time measurements of gap states are described.

2.2 HIGH-FREQUENCY CAPACITANCE-VOLTAGE METHOD[15]

When the capacitance of an undoped a-Si films is measured at a high frequency, *e.g.*, 1 MHz, the ionization of gap states cannot follow the measurement frequency, and the a-Si films can be considered to be dielectrics which in the capacitance is determined simply by the dielectric constant and geometric size. The differential capacitance of metal/a-Si/n-type crystalline Si (c-Si) structure at high frequency is given by the series capacitance of the a-Si films and the n-type c-Si space charge layer which can be calculated in terms of the voltage across the c-Si space charge layer, ψ_c. Thus, from the measured capacitance of the metal/a-Si/n-type c-Si structure, the voltage across the c-Si space charge layer, ψ_c, can be determined.

The energy-band diagram of a CVD a-Si/c-Si junction at thermal equilibrium can be determined from the high-frequency capacitance at zero bias and is shown in Fig.2.1.[15] The blocking barrier for electrons in the c-Si conduction band is formed by the mobility gap of CVD a-Si, and negative space charge in the c-Si space charge layer, Q_c, is formed by accumulated electrons in the c-Si conduction band.

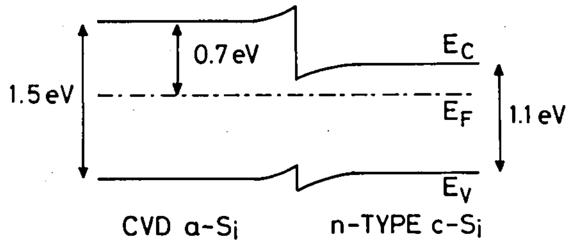

FIGURE 2.1 Energy-band diagram of CVD a-Si/n-type crystalline Si junctions at thermal equilibrium.

On the other hand, positive space charge in the a-Si space charge layer, Q_a, is formed by positively charged gap states in the a-Si and equals $-Q_c$. The relation $Q_a + Q_c = 0$ remains valid even after application of voltage to the junctions.[15] Figure 2.2 shows space charge and potential distributions in CVD a-Si/n-type c-Si junctions schematically. In each junction, the following expression is expected:

$$V = \psi_a + \psi_c + V_{FB}, \tag{2.1}$$

where V_{FB} is the flat-band voltage, *i.e.*, the applied voltage which makes ψ_c zero. The differential capacitances of c-Si at $\psi_c = 0$ and of

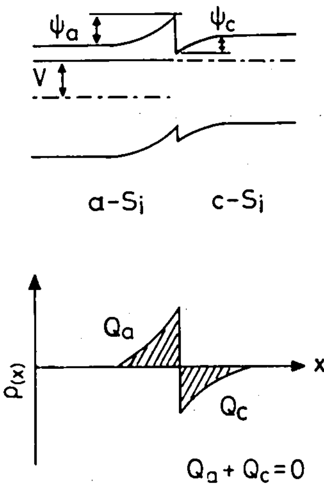

FIGURE 2.2
Potential distribution and space charge distribution in a positively biased CVD a-Si/n-type crystalline Si junction.

an a-Si film can then be calculated, and V_{FB} is determined by the experimental *C-V* characteristic. From the measured capacitance after application of a voltage V, ψ_c can be obtained and then ψ_a is evaluated from Eq.(2.1). Since the space charge Q_c can be calculated from ψ_c , Q_a is obtained as a function of ψ_a. From the relationship between Q_a and ψ_a, the gap-state density is obtained without assuming the potential distribution in an a-Si space charge layer.[15]

2.3 FIELD-EFFECT METHOD FOR CVD a-Si

The field effect of CVD a-Si was measured in the structure shown in Fig.2.3. Since CVD a-Si contains a high gap-state density, a high electric field must be applied to the insulator, and the leakage current through the insulator affects the field-effect measurements. Thus, interdigitated geometry was used for source and drain electrodes. Figure 2.4 shows typical field-effect results on CVD a-Si at several temperatures. The U-shaped characteristic appears in the field effect and implies that the CVD a-Si film is intrinsic. This characteristic is believed to originate from hopping conduction. The dark conductivity of CVD a-Si above room temperature is given by

$$\sigma = \sigma_1 \exp\left(-\frac{0.7\mathrm{eV}}{k_B T}\right) + \sigma_2 \exp\left(-\frac{0.15\mathrm{eV}}{k_B T}\right) , \qquad (2.2)$$

where the first term arises from extended-state conduction and the second term from hopping conduction. The relative contribution of

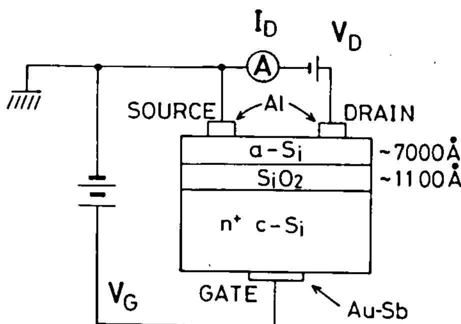

FIGURE 2.3

Sample structure and experimental set-up for field-effect measurements.

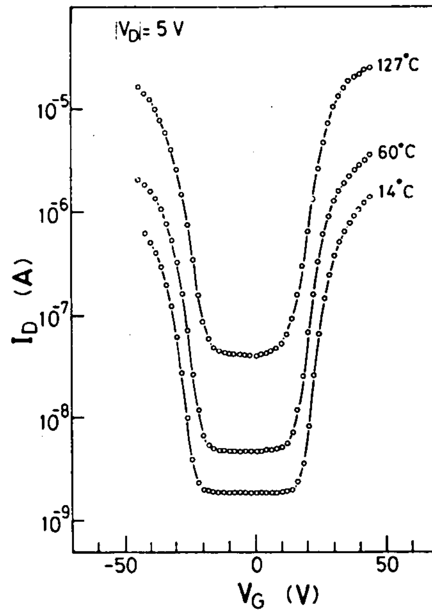

FIGURE 2.4 Typical field effect of CVD a-Si measured at various temperatures. The film was deposited using a mixture in which silane gas concentration in argon was 0.2%.

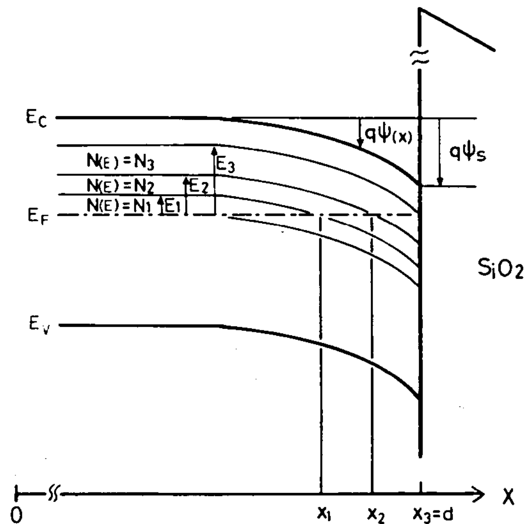

FIGURE 2.5 Definition of x_i in the calculation of source-drain conductance.

hopping conduction decreases with increasing temperature. This reduction is also expected in the field effect. Actually, the drain current changes even at small gate voltages at elevated temperatures, as shown in Fig.2.4. Since it is desirable to reduce the contribution of hopping conduction to field-effect data, elevation of the measurement temperature in field-effect method on CVD a-Si is useful.

The gap-state density can then be derived by a numerical analysis, as follows. The gap-state density distribution is assumed to be

$$N_{(E)} = N_i \qquad \text{at } E_{i-1} < E - E_F < E_i \text{ ,} \tag{2.3}$$

where E_0 is zero, and i is an integer. We consider the a-Si space-charge layer in which the potential distribution is denoted by $\psi_{(x)}$. As shown in Fig.2.5, x_i is defined by

$$q\,\psi_{(x_i)} = E_i \text{ .} \tag{2.4}$$

For $x_{i-1} \leqq x \leqq x_i$ $(i \geqq 2)$, the Poisson equation becomes

$$\frac{d^2\psi_{(x)}}{dx^2} = A_i\,\psi_{(x)} + B_i \text{ ,} \tag{2.5}$$

where

$$A_i = \frac{q^2 N_i}{\varepsilon_a \varepsilon_0} \quad \text{and} \quad B_i = \frac{q}{\varepsilon_a \varepsilon_0} \sum_{j=1}^{i-1} (E_j - E_{j-1})\,N_j \text{ .}$$

Integration of Eq.(2.5) yields

$$\psi_{(x)} = C_1 \exp\{\sqrt{A_i}(x - x_i)\} + C_2 \exp\{-\sqrt{A_i}(x - x_i)\} - \frac{B_i}{A_i} \text{ ,} \tag{2.6}$$

where

$$C_1 = \frac{1}{2}\left(\psi_{(x_i)} - \frac{F_i}{\sqrt{A_i}} + \frac{B_i}{A_i}\right) , \quad C_2 = \frac{1}{2}\left(\psi_{(x_i)} + \frac{F_i}{\sqrt{A_i}} + \frac{B_i}{A_i}\right) ,$$

and F_i denotes the electric field at $x = x_i$.
For the region of $0 \leqq x \leqq x_1$, we have

$$\psi_{(x)} = \psi_{(x_1)} \exp\{\sqrt{A_1}(x - x_1)\} . \tag{2.7}$$

The conductivity $\sigma_{(x)}$ is assumed to have the form

$$\sigma_{(x)} = \sigma_1 \exp\left(-\frac{E_c - E_F - q\psi_{(x)}}{k_B T}\right) + \sigma_2 \exp\left(-\frac{E_H}{k_B T}\right) , \tag{2.8}$$

and the source-drain conductance G is given by

$$G = \frac{W}{L}\int_0^{\mathrm{d}} \sigma_{(x)}\, \mathrm{d}x , \tag{2.9}$$

where W and L are the width of and the gap between the source and drain electrodes, respectively. The electric field at $x = d$, F_s, is obtained from differentiation of $\psi_{(x)}$, and gives the space charge density Q_s. Thus,

$$Q_s = \varepsilon_{\mathrm{a}} \varepsilon_0 F_s = -\varepsilon_{\mathrm{a}} \varepsilon_0 \left.\frac{\mathrm{d}\psi_{(x)}}{\mathrm{d}x}\right|_{x=d} . \tag{2.10}$$

G and Q_s can be calculated numerically by Eqs.(2.6)-(2.10), provided N_i and ψ_s $(= \psi_{(d)})$ are known. On the other hand, G and Q_s can be obtained experimentally, since Q_s is given by

$$Q_s = \frac{\varepsilon_{\mathrm{ox}} \varepsilon_0}{d_{ox}} (V_G - V_{FB} - \psi_{\mathrm{s}}) , \tag{2.11}$$

where $\varepsilon_{\mathrm{ox}}$ and d_{ox} are the dielectric constant and thickness of the oxide film, respectively. The sets of N_i and ψ_{s} which make G and Q_s consistent with the experimental results can be determined by a computer analysis.

2.4 RESULTS ON GAP-STATE DENSITY OF CVD a-Si

The gap-state densities in CVD a-Si films deposited at 550°C from two SiH_4/Ar gaseous mixtures are shown in Fig.2.6. The results near the Fermi level were determined by the high-frequency *C-V* method, and those far from E_F the field-effect method. It appears that the minimum gap-state density of CVD a-Si is $2 \sim 5 \times 10^{17}$ $cm^{-3}eV^{-1}$. The increase of the gap-state density above $E_F + 0.4$ eV and below $E_F - 0.4$ eV might result from the tail states or the weak bonds between Si atoms.[16] The gap states at $E_F - 0.3$ eV $< E < E_F + 0.35$ eV seem to originate from the dangling bonds. It has been considered that the dangling bond states locate near the mid-gap.[17-21] The density of dangling bonds in CVD a-Si is reported to be the order of 10^{18} cm^{-3},[16] which agrees with the integrated density of gap states shown in the figure with respect to their energies.

2.5 MIS CAPACITANCE-FREQUENCY-TEMPERATURE MEASUREMENT[22]

The gap-state density around the Fermi level and their capture cross section can be evaluated from frequency and temperature dependence of the flat-band capacitance of MIS diodes in which an

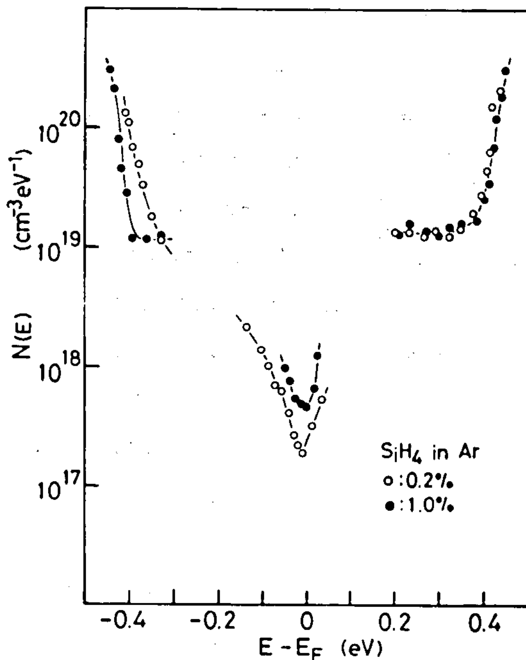

FIGURE 2.6

Gap-state densities in CVD a-Si films deposited at 550°C.

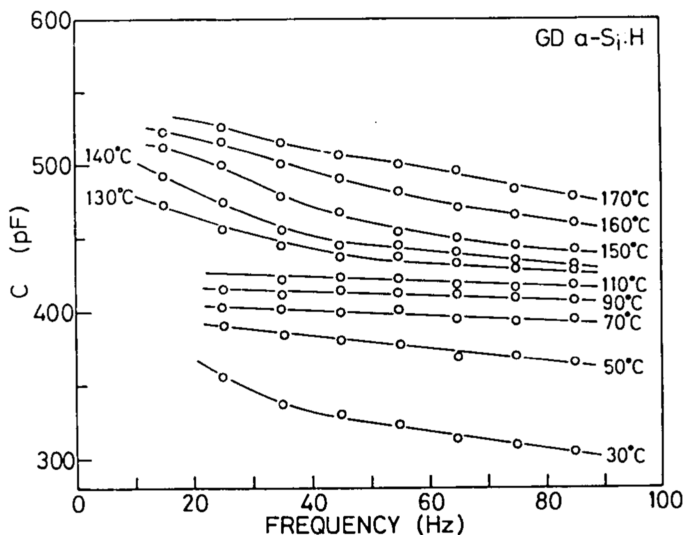

FIGURE 2.7 Frequency and temperature dependence of flat-band capacitance of a GD a-Si:H MIS diode.

a-Si film is used as semiconductor.

Figure 2.7 shows the flat-band capacitance of the a-Si:H MIS diode, in which 0.6-μm-thick GD a-Si:H film is deposited at 250°C onto 0.37-μm-thick GD a-SiN insulator on crystalline Si substrate, measured at various frequencies and temperatures.

The contribution of a-Si:H neutral bulk region to a measured capacitance for frequencies below 100 Hz can be eliminated by elevation of measurement temperature above 80°C, and the contribution of free carriers in the extended states to the MIS flat-band capacitance is negligibly small.[22] Thus, the contribution of a-Si film to the MIS diode capacitance could be dominated by charging and discharging of traps at interface and/or in a-Si:H space-charge layer. Since the insulator is dielectric, variations in the MIS diode capacitance with temperature or frequency could be associated with a variation of the number of responsible traps to measurement frequency at a specific temperature.

The results shown in Fig.2.7 can be well understood by assuming that the fast trapping state fully responsible to 100 Hz at 110°C

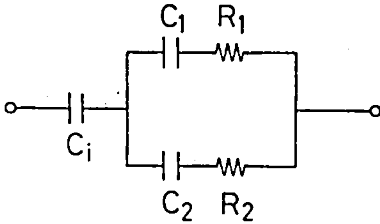

FIGURE 2.8
Equivalent circuit for flat-band capacitance of a-Si MIS diodes.

and the slow trapping states partly responsible to 20∿100 Hz above 130°C. The response time of slow trapping states can be evaluated from the results shown in Fig.2.7 by an analysis assumig an equivalent circuit shown in Fig.2.8. The response time of slow trapping states in the MIS diode is shown in Fig.2.9. The activation energy in the temperature dependence of response time is 0.72 eV, which agrees with the activation energy of dark conductivity of 0.75 eV. This suggests that trapping of free carriers by the slow states is due to states around the Fermi level, since the activation energy of dark conductivity would represent the energy difference between the electron mobility edge and the Fermi level. In contrast, the response time of slow states in metal/SiO_2/CVD a-Si:N diodes has the activation energy of 0.63 eV, which is smaller by 0.1 eV than the activation energy of dark conductivity. In this case, the trapping by slow states might be by ways of tail states around 0.1 eV below the

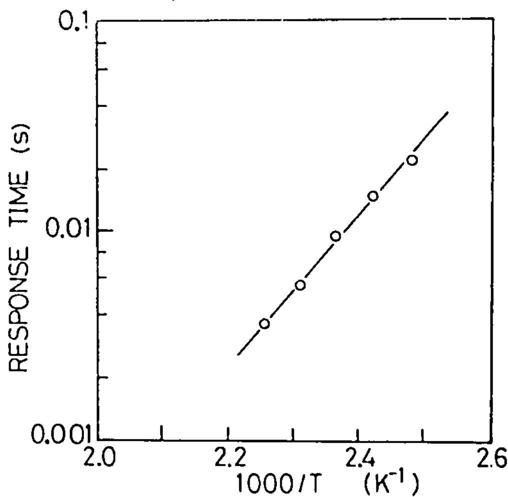

FIGURE 2.9
Response time of slow states in GD a-Si:H MIS diodes.

electron mobility edge in CVD a-Si:N films. Provided the density of states around the mobility edge of 10^{20} $cm^{-3}eV^{-1}$ and the electron thermal velocity of 10^{7} cm/s, the capture cross section of slow states can be deduced to be 10^{-15} cm^{2} in a GD a-Si:H MIS diode and 10^{-17} cm^{2} in a CVD a-Si:N MIS diode. The density of trapping states could be evaluated by assuming that these traps originate from the bulk gap states or interface states. The results are summarized in Table 2.2. It is noted that the trap densities of slow and fast states in a GD a-Si:H MIS diode are remarkably smaller than those in a CVD a-Si:N MIS diode.

2.6 SUMMARY

In order to understand detailed electronic processes in a-Si and its alloys, characterization method of the gap states has to be established. As reviewed in this chapter, reported measurements of the gap-state density include any disadvantage. Especially, most of reported measurement techniques are not available to reliable measurements of the gap-state density in CVD a-Si. In this chapter, new measurement method and improved method of the gap-state density in CVD a-Si films have been proposed and demonstrated. The reponse time and density of traps in MIS diodes having GD a-Si:H and CVD a-Si:N films as semiconductor, which originate from the gap states or interface states, have been evaluated from frequency and temperature dependence of flat-band capacitance of the diodes. The results in

TABLE 2.2 Trap densities in a-Si MIS diodes.

	GD a-Si:H MNS	CVD a-Si:N MOS	
BULK GAP STATES:			
FAST STATES	7×10^{15}	6×10^{17}	$(cm^{-3}eV^{-1})$
SLOW STATES	2×10^{16}	$0.6 \sim 2 \times 10^{19}$	$(cm^{-3}eV^{-1})$
INTERFACE STATES:			
FAST STATES	2×10^{11}	3×10^{11}	$(cm^{-2}eV^{-1})$
SLOW STATES	7×10^{11}	$0.6 \sim 1 \times 10^{13}$	$(cm^{-2}eV^{-1})$

this chapter can be summarized as follows.

(i) The gap-state density in CVD a-Si films at 550°C has a minimum around the Fermi level of $2 \sim 5 \times 10^{17}$ $cm^{-3}eV^{-1}$ and rapidly increases away from the Fermi level. The gap-state density reaches the order of 10^{20} $cm^{-3}eV^{-1}$ at $E - E_F = \pm 0.4$ eV.

(ii) The response time and density of traps in MIS structures have been evaluated from frequecy and temperature dependence of the MIS diode flat-band capacitance. It has been found that the GD a-Si:H and CVD a-Si:N MIS diodes contain slow and fast trapping states at the interface and/or the bulk.

(iii) The response time of slow states was found to be 2.5×10^{-11} $\exp(0.72\mathrm{eV}/k_B T)$ s and $2.4 \times 10^{-9} \exp(0.6\mathrm{eV}/k_B T)$ s for GD a-Si:H and CVD a-Si:N MIS diodes, respectively.

(iv) The trap densities of fast and slow states were found to be 7×10^{15} $cm^{-3}eV^{-1}$ and 2×10^{16} $cm^{-3}eV^{-1}$ for GD a-Si:H MIS diodes, and 6×10^{17} $cm^{-3}eV^{-1}$ and 6×10^{18} to 2×10^{19} $cm^{-3}eV^{-1}$ for CVD a-Si:N MIS diodes, respectively, provided these states originate from bulk gap states.

(v) Provided from interface states, the trap densities of fast and slow states were found to be 2×10^{11} $cm^{-2}eV^{-1}$ and 3×10^{11} $cm^{-2}eV^{-1}$ for GD a-Si:H MIS diodes, and 7×10^{11} $cm^{-2}eV^{-1}$ and 6×10^{12} to 1×10^{13} $cm^{-2}eV^{-1}$ for CVD a-Si:N MIS diodes, respectively.

REFERENCES

1) N.F. Mott, Philos. Mag., 19 (1969) 835.

2) W.E. Spear and P.G. LeComber, J. Non-Cryst. Solids, 8-10 (1972) 727.

3) A. Madan, P.G. LeComber, and W.E. Spear, J. Non-Cryst. Solids, 20 (1976) 239.

4) N.B. Goodman and H. Fritzsche, Philos. Mag., B42 (1980) 149.

5) N.B. Goodman, Philos. Mag., B45 (1982) 407.

6) T. Nakashita, M. Hirose, and Y. Osaka, Jpn. J. Appl. Phys., 17 (1978) 985.

7) I. Balberg and D.E. Carlson, Phys. Rev. Lett., 58 (1979) 58.
8) M. Hirose, T. Suzuki, and D.H. Döhler, Appl. Phys. Lett., 34 (1979) 234.
9) J.D. Cohen, D.V. Lang, and J.P. Harbison, Phys. Rev. Lett., 45 (1980) 197.
10) H. Okushi, Y. Tokumaru, S. Yamasaki, H. Oheda, and K. Tanaka, Jpn. J. Appl. Phys., 20 (1981) L549.
11) P. Viktorovitch and B. Moddel, J. Appl. Phys., 51 (1980) 4847.
12) P. Viktorovitch, J. Appl. Phys., 52 (1981) 1392.
13) S. Guha, Solar Energy Materials, 8 (1982) 269.
14) T. Suzuki, M. Hirose, M. Ueda, and Y. Osaka, Solar Energy Materials, 8 (1982) 285.
15) G. Sasaki, S. Fujita, and A. Sasaki, J. Appl. Phys., 53 (1982) 1013; *and see also Appendix.*
16) S. Hasegawa, T. Kasajima, and T. Shimizu, Philos. Mag., B43 (1981) 149.
17) K. Morigaki, Y. Sano, and I. Hirabayashi, Solid State Commun., 39 (1981) 947.
18) K. Morigaki, Y. Sano, and I. Hirabayashi, J. Phys. Soc. Japan, 51 (1982) 147.
19) H. Derch, J. Stuke, and J. Beicher, Phys. Stat. Solidi, (b)105 (1981) 265.
20) J.D. Cohen, J.P. Harbison, and K.W. Wecht, Phys. Rev. Lett., 48 (1981) 109.
21) W.B. Jackson, Solid State Commun., 44 (1979) 13.
22) G. Sasaki, S. Fujita, and A. Sasaki, J. Appl. Phys., 29 (1983) 4008, *and see also Appendix.*

III. CHEMICAL VAPOR DEPOSITION OF AMORPHOUS SILICON-NITROGEN ALLOYS

3.1 INTRODUCTION

Chemical vapor deposition (CVD) is widely used in the industrial field of solid-state electronic devices. Epitaxial layers of crystalline Si can be grown by the thermal decomposition of silane gas (SiH_4)[1] and insulator films of SiO_2 or Si_3N_4 can be deposited by the thermal reactions of SiH_4 with O_2,[2] NO_x,[3] CO_2, or NH_3.[4] The silane gas is thermally decomposed into Si atoms above 500°C which are deposited onto a substrate and form Si films.[5] The Si films deposited below 650°C are amorphous.[6] The deposition mechanism of CVD Si films from SiH_4 gas is not fully understood but discussed in terms of either the homogeneous reaction model[7-9] in which the gas phase reaction is the rate-limiting step or the heterogeneous reaction model[10-13] in which the surface reaction is the rate-limiting step.

Si_3N_4 films can be thermally deposited by the reaction of SiH_4 and NH_3 gases above the deposition temperature of 700°C.[4,14-16] The films deposited below 900°C are amorphous.[14] The deposition rate is decreased, relative to the rate of a-Si films, by a little incorporation of NH_3 gas into the reactant gas and saturated by a further incorporation of NH_3 gas, where the films deposited at a little flow of NH_3 gas is Si-rich.[14] Moreover, the deposition rate is rapidly decreased by lowering the deposition temperature with the activation energy of 2.2 eV below 900°C.[14]

In this chapter, preparation of CVD amorphous silicon-nitrogen (a-Si:N or a-SiN_x) films from SiH_4, NH_3, and Ar gases at 550°C is described. The deposition mechanism of CVD a-Si:N films and the incorporation mechanism of nitrogen into a film are also described.

3.2 PREPARATION

The CVD reactor in this study is a conventional resistance-heated quartz tube reactor. The deposition gas-pressure and temperature are atmospheric and 550°C, respectively. Since the reactor is

a hot-wall type, the quartz tube and susceptor are contaminated by deposits after the film deposition. These contaminated instruments were cleaned by HF-HNO_3 acid etching, purified water and acetone rinse. After these chemical cleaning, the instruments were baked at 950°C for 2 hrs.

The reactant gas flows were controlled by a mass flow controller for SiH_4 gas and rotameters for Ar and NH_3 gases. The SiH_4 gas flow could be controlled within ±0.2 sccm. The Ar gas was deoxidized and demoistened by an inert gas purifier. The SiH_4 gas was supplied by a pure gas. The NH_3 gas was supplied by a 100 ppm, 1% Ar-diluted, or pure gas. The total gas flow rate was maintained at 1 ℓ/min, which could yield the reactant gas flow of about 6 cm/s above substrates.

Substrates were fused quartz, crystalline Si, and thermally oxidized crystalline Si, where films on fused quartz were used for characterization of optical and electrical properties, films on crystalline Si for measurements of infrared absorption, and thermally oxidized crystalline Si for electrical measurements of metal/insulator/semiconductor (MIS) diodes. Fused quartz and crystalline Si substrates were cleaned by trichloroethylene and acetone, and boiled in H_2SO_4 and HNO_3 acids successively. The cleaned and boiled crystalline Si substrates were etched by diluted HF acid. Thermally oxidized crystalline Si substrates were prepared in the CVD reactor by dry oxidation at 950°C. After the oxidation, the oxygen gas in the reactor was eliminated by a vacuum pump.

When films were deposited onto fused quartz at a high NH_3 gas concentration $[NH_3]$, cracks were observed in the films, *e.g.*, in films of thickness $d = 0.3$ μm deposited by the silane gas concentration $[SiH_4] = 0.05\%$ and $[NH_3] = 0.33\%$ and $d = 0.6$ μm by $[SiH_4] = 0.2\%$ and $[NH_3] = 0.33\%$. These cracks are considered to originate from the differences in thermal expansion coefficients between the quartz substrates and films which contain many nitrogen atoms. The electrical properties of these films were not investigated. It was confirm-

ed by the X-ray diffraction that the films were amorphous.

3.3 DEPOSITION RATE

Figure 3.1 shows the deposition rate of undoped CVD a-Si films at 550°C under various SiH_4 gas concentrations $[SiH_4]$. As shown in the figure, the deposition rate is approximately proportional to $[SiH_4]$. Figure 3.2 shows the deposition rate of CVD a-Si:N films at 550°C under various SiH_4 and NH_3 gas concentrations. The deposition rate is drastically decreased by the high NH_3 gas introduction into the reactant gas. Similar reduction of the deposition rate was also reported on PH_3 or AsH_3 incorporation into the reactant gas for CVD Si films.[17,18]

It has been proposed that the thermal deposition of Si films from SiH_4 gas below 700°C consists of the elemental reactions of:[12,13]
(i) the gas phase decomposition of SiH_4, *i.e.*,

$$SiH_4 \underset{k_{-1}}{\overset{k_1}{\rightleftarrows}} SiH_2 + H_2 , \qquad (3.1)$$

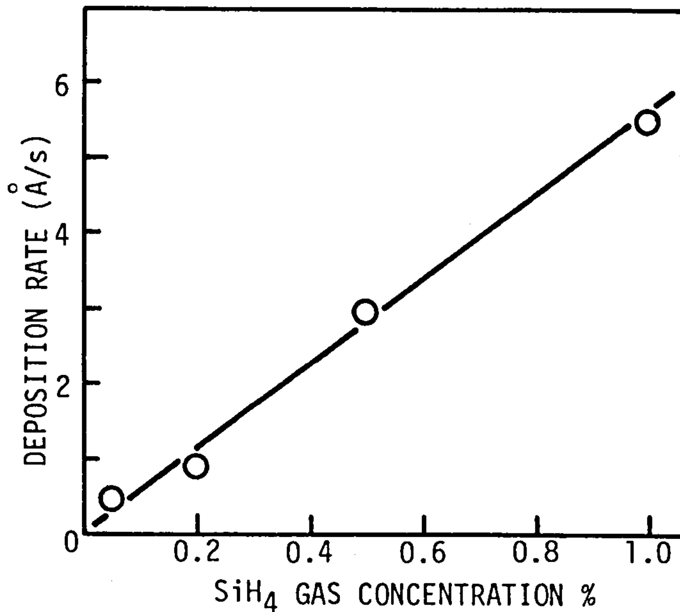

FIGURE 3.1 Deposition rate of undoped CVD a-Si films at 550°C.

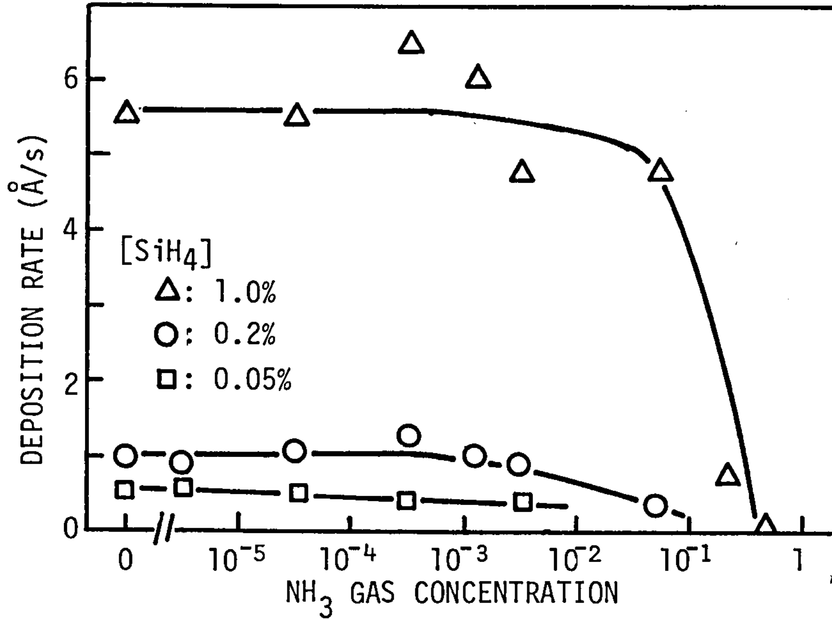

FIGURE 3.2 Deposition rate of CVD a-Si:N films at 550°C.

(ii) the adsorption of SiH_2, *i.e.*,

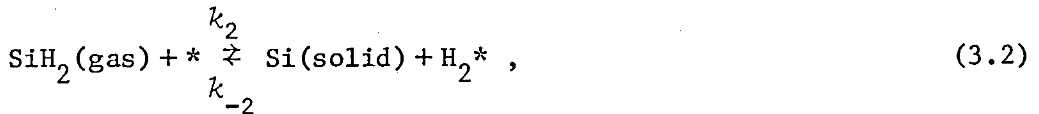

$$SiH_2(\text{gas}) + * \underset{k_{-2}}{\overset{k_2}{\rightleftarrows}} Si(\text{solid}) + H_2* \ , \tag{3.2}$$

and (iii) the desorption of H_2, *i.e.*,

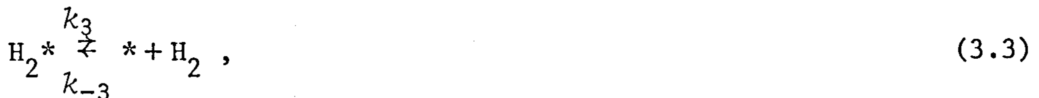

$$H_2* \underset{k_{-3}}{\overset{k_3}{\rightleftarrows}} * + H_2 \ , \tag{3.3}$$

where * denotes the adsorption site at surface, H_2* the H_2 molecules adsorbed to surface, and k the rate constant. Provided the rate-limiting step, the deposition rate R could be derived and is summarized in Table 3.1, where the poor decomposion of SiH_4, which yields $[SiH_2] = \sqrt{K_1[SiH_4]}$, is assumed for the derivations of R_2 and R_3. If and only if R_i ($i = 1,2,$ and 3) is the smallest among the deposition rate summarized in Table 3.1, the i-th reaction step could limit the deposition rate. As shown in Table 3.1, the deposition rate R_1 is

TABLE 3.1 Dependence of deposition rate R on silane gas concentration $[SiH_4]$. K, the equilibrium constant.

RATE-LIMITING STEP	DEPOSITION RATE
(i) SiH_4 DECOMPOSITION	$R_1 = k_1 [SiH_4]$
(ii) SiH_2 ADSORPTION	$R_2 = k_2\sqrt{K_1[SiH_4]}[*]$
(iii) H_2 DESORPTION	$R_3 = k_3 K_2\sqrt{K_1[SiH_4]}[*]$

proportional to $[SiH_4]$, whereas R_2 and R_3 are proportional to $\sqrt{[SiH_4]}$. Therefore, the experimental results shown in Fig.3.1 could be understood by that the gas phase decomposition of SiH_4 limits the deposition rate of undoped CVD a-Si films.

It is reported that the nitrogen incorporation into a-Si:H films suppresses the hydrogen effusion by thermal annealing.[19] Thus, the nitrogen incorporation into CVD a-Si would suppress the hydrogen desorption during deposition, which would yield a decrease of the rate constant k_3. Since the deposition rate R_3 is proportional to k_3 , R_3 is decreased by decreases of k_3. When k_3 is so decreased that R_3 is smaller than R_1, the rate-limiting step in film deposition would be changed from the gas phase decomposition step to the hydrogen desorption step. The nitrogen incorporation exceeding such threshold that $R_1 = R_3$ would decrease monotonically the deposition rate. As shown in Fig.3.2, the deposition rate of CVD a-Si:N films is decreased by the NH_3 incorporation into the reactant gas of which the concentration exceeds around 20% at $[SiH_4] = 1.0\%$ or around 5% at $[SiH_4] = 0.2\%$. Such decreases of the deposition rate could be understood by the suppression of hydrogen desorption due to the nitrogen incorporation. The larger threshold of NH_3 gas concentration, at which the deposition rate begins to decrease, of films at $[SiH_4] =$ 1.0% than that of films at $[SiH_4] = 0.2\%$ would originate from fewer incorporated nitrogen atoms as described in the next section.

3.4 INFRARED ABSORPTION AND NITROGEN CONTENT

The films prepared at large ($[NH_3]/[SiH_4]$)-ratios on crystalline Si substrates showed absorption near 800 cm^{-1} in the infrared transmittance, although no absorption due to Si-H ($\simeq$ 2000 cm^{-1}), Si-O ($\simeq$ 1100 cm^{-1}), or N-H ($\simeq$ 1200 cm^{-1}) was detected. Figure 3.3 shows typical infrared absorption characteristics of a-Si:N and CVD a-Si_3N_4 at 700°C.[20] The maximum absorption wavenumber for the Si-N bond oscillation was reported to be 935 cm^{-1} in crystalline Si_3N_4 powder[4,21] and around 850 cm^{-1} in amorphous Si_3N_4 prepared by glow discharge, reactive sputtering, and chemical vapor deposition.[21] The peak shift from 850 cm^{-1} in a-Si_3N_4 to 800 cm^{-1} in a-Si:N would result from the difference in the atomic environments around the Si-N oscillators.

Since it is considered that these absorption bands are due to vibrations of Si-N bonds, the integrated absorption coefficient over the absorption band, S_a (cm^{-1}), is considered to be proportional to the incorporated nitrogen content C_N (cm^{-3}). Here, S_a is defined by

$$S_a = \int \frac{\alpha}{\nu} d\nu \ , \tag{3.4}$$

in which each nitrogen atom is assumed to bond three silicon atoms. Here, ν denotes the wavenumber in the Si-N absorption band. Since the density and the absorption coefficient in the Si-N absorption band were reported on CVD a-Si_3N_4 films,[22] a proportional constant between C_N and S_a could be obtained. Then, the nitrogen content C_N can be derived from S_a by

$$C_N = 7.73 \times 10^{18} S_a \quad (cm^{-3}). \tag{3.5}$$

The mole fraction of nitrogen atoms to silicon atoms, x, could be deduced roughly by assuming the concentration of Si atoms in films. The number of Si atoms in CVD a-Si or Si_3N_4 can be calculated from the densities reported in literature[3,22] and is estimated as 5×10^{22} cm^{-3} in a CVD a-Si film or 4×10^{22} cm^{-3} in an a-Si_3N_4 film.

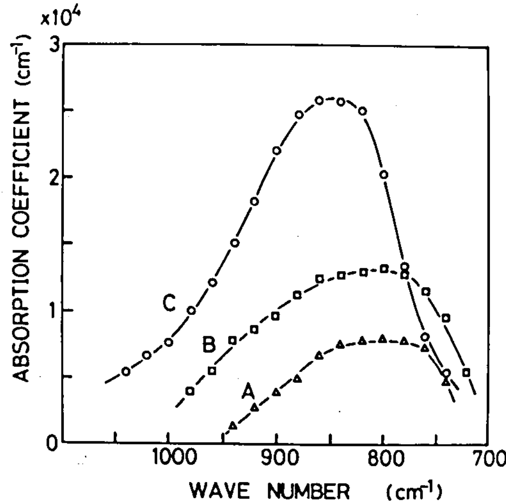

FIGURE 3.3 Infrared absorption spectra of a-Si:N films (A), (B), and a-Si_3N_4 film (C). (A) $[SiH_4] = 0.2\%$, $[NH_3] = 0.03\%$ at 550°C. (B) $[SiH_4] = 0.05\%$, $[NH_3] = 0.33\%$ at 550°C. (C) deposited at 700°C.

Then, with the assumption that the number of Si atoms in a-SiN_x varies linearly with respect to x, the mole fraction of nitrogen atoms to silicon, x, can be evaluated as[23]

$$x = \frac{1}{3}\{10 - (100 - 1.2 \times 10^{-21} C_N)^{1/2}\}. \tag{3.6}$$

Figure 3.4 shows the nitrogen content in films deposited at various SiH_4 and NH_3 gas concentrations. The nitrogen content tends to saturate with increases of the NH_3 gas concentration. If the nitrogen incorporation into films is due to the heterogeneous reaction, *i.e.*, the catalytic reaction at surface, the over-all reaction would consist of the elemental steps of:

(i) the adsorption of NH_3 molecules, *i.e.*,

$$NH_3 + * \underset{k_{-4}}{\overset{k_4}{\rightleftarrows}} NH_3^* , \tag{3.7}$$

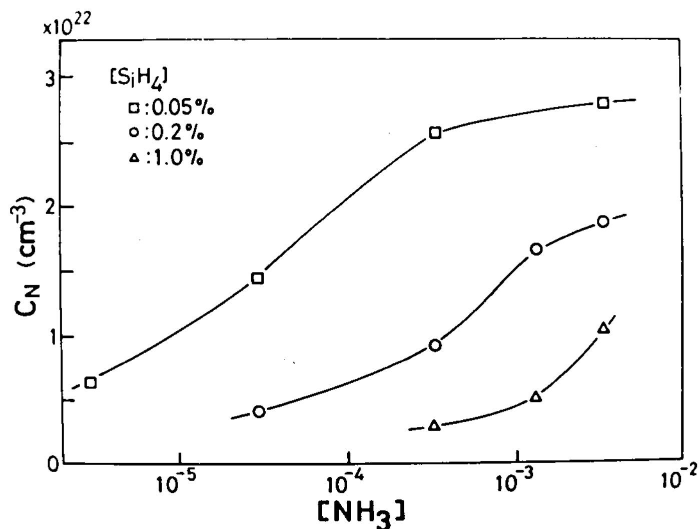

FIGURE 3.4 Incorporated nitrogen content of a-Si:N films evaluated from integrated absorption coefficient.

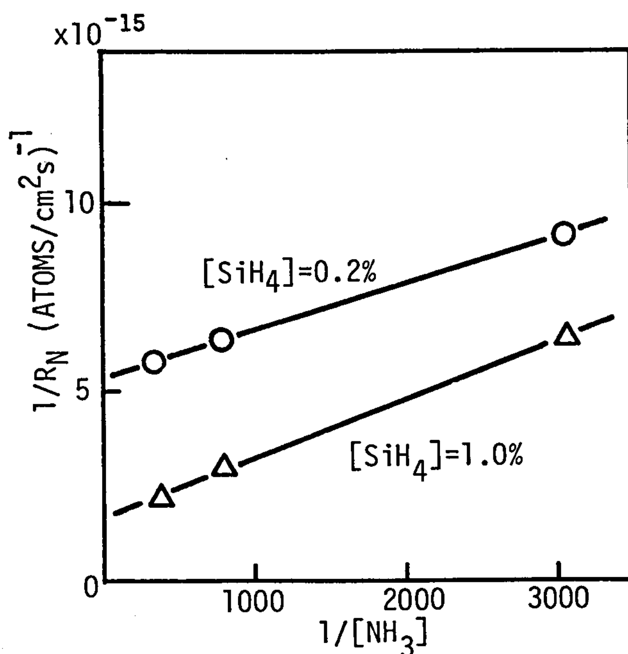

FIGURE 3.5 Relation between the inverse of nitrogen incorporation rate and the inverse of NH_3 gas concentration.

and (ii) the decomposition of adsorbed NH_3, or desorption of H, *i.e.*,

$$NH_3{*} \underset{k_{-5}}{\overset{k_5}{\rightleftarrows}} N + * + \frac{3}{2}H_2 . \tag{3.8}$$

If the incorporation of nitrogen was limited by the adsorption of NH_3 molecules, the nitrogen incorporation rate R_N (atoms/cm^{2}s), which is equal to the product of the nitrogen content and the deposition rate, would be $k_4[NH_3][*]$, which was not approved by the experimental results, since the nitrogen incorporation is saturated with $[NH_3]$. If the decomposition of adsorbed NH_3 molecules is the rate-limiting step, the nitrogen incorporation rate R_N could be represented by[23]

$$R_N = \frac{k_5 N_s}{1 + (K_4[NH_3])^{-1}} , \tag{3.9}$$

where N_s is the number of adsorption site and equal to the sum of the numbers of available adsorption site [*] and adsorbed NH_3 molecules $[NH_3*]$. The expression on R_N implies the linear relation between the inverse of R_N and the inverse of $[NH_3]$. Figure 3.5 shows the relation between $1/R_N$ and $1/[NH_3]$ on CVD a-Si:N films, which shows the good linear relation between them. Therefore, the nitrogen incorporation rate would be limited by the decomposition of adsorbed NH_3 molecules, provided the heterogeneous reaction.

3.5 SUMMARY

Preparation of a-Si:N films by chemical vapor deposition at 550° C from SiH_4, NH_3, and Ar gases has been described. The deposition rate, incorporated nitrogen content, and the nitrogen incorporation rate of the films were measured and discussed. Their results can be summarized as follows.

(i) The deposition rate of undoped CVD a-Si films is proportional to the SiH_4 gas concentration, which suggests that the gas phase decomposition of SiH_4 molecules would limit the deposition rate.

(ii) The NH_3 gas introduction into reactant gas remarkably decreases

the deposition rate, and films are hardly deposited from the reactant gas of which the NH_3 gas concentration exceeds 20%. These results might be understood by that the hydrogen desorption from the adsorption sites at surface during the deposition is suppressed by the nitrogen incorporation into films.

(iii) The incorporated nitrogen content in films was evaluated by the infrared absorption around 800 cm^{-1}. The nitrogen content increases with increases of the NH_3 gas concentration and/or decreases of the SiH_4 gas concentration.

(iv) The nitrogen incorporation rate of films could be explained by the heterogeneous reaction of NH_3 molecules in which the decomposition of adsorbed NH_3 molecules is the rate-limiting step.

REFERENCES

1) S.R. Bhola and A. Mayer, RCA Rev., 24 (1963) 511.
2) N. Goldsmith and W. Kern, RCA Rev., 31 (1970) 153.
3) D.M. Brown, P.V. Gray, F.K. Henman, H.R. Phillip, and E.A. Taft, J. Electrochem. Soc., 115 (1968) 311.
4) S.M. Hu, J. Electrochem. Soc., 113 (1966) 693.
5) C.H. Lewis, H.C. Kelly, M.B. Giusto, and S. Johnson, J. Electrochem. Soc., 108 (1961) 1114.
6) R.M. Anderson, J. Electrochem. Soc., 120 (1973) 1540.
7) F.C. Eversteijn, Philips Res. Rep., 26 (1971) 134.
8) K.J. Sladek, J. Electrochem. Soc., 118 (1971) 654.
9) B.A. Scott, D.M. Plecenic, and E.E. Simonyi, Appl. Phys. Lett., 39 (1981) 73.
10) J.Y.W. Seto, J. Electrochem. Soc., 122 (1975) 701.
11) W.A. Bryant, Thin Solid Films, 60 (1979) 19.
12) W.A.P. Claassen and J. Bloem, J. Crystal Growth, 51 (1981) 443.
13) W.A.P. Claassedn, J. Bloem, W.G.J.N. Valkenburg, and C.H.J. van den Brekel, J. Crystal Growth, 57 (1982) 259.
14) K.E. Bean, P.S. Gleim, R.L. Yeakley, and W.R. Runyan, J. Electrochem. Soc., 114 (1967) 733.

15) V.Y. Doo, D.R. Kerr, and D.R. Nichols, J. Electrochem. Soc. 115 (1968) 61.

16) J.R. Yeargan and H.L. Tayler, J. Electrochem. Soc., 115 (19
273.

17) R.F.C. Farrow and J.D. Filby, J. Electrochem. Soc., 118 (19
149.

18) M. Taniguchi, M. Hirose, and Y. Osaka, J. Crystal Growth, 4
(1978) 126.

19) M. Kumeda, S. Oozora, N. Ishii, A. Morimoto, and T. Shimizu, IECE Japan Rept. Tech. Group Electron Devices, ED82-65 (1982 (*in Japanese*).

20) S. Fujita, H. Toyoshima, M. Nishihara, and A. Sasaki, J. El
tron. Mat., 11 (1982) 795.

21) E.A. Taft, J. Electrochem. Soc., 118 (1971) 1341.

22) M. Hirose, M. Taniguchi, and Y. Osaka, *Proc. 7th Int. Conf. Amorphous & Liquid Semiconductors, Edinburgh, 1977* (Center f
Industrial Consultancy and Liaison, University of Edinburgh, 1977) p.352.

23) *See Appendix*.

IV. OPTICAL PROPERTIES OF CHEMICALLY VAPOR-DEPOSITED AMORPHOUS SILICON-NITROGEN ALLOYS

4.1 INTRODUCTION

One of important differences between metals and semiconductors is that semiconductors are transparent for photons of which the energy is lower than the energy of the band gap. It is understood that dominant optical absorption in semiconductors is due to electron excitation from the valence band to the conduction band. Amorphous Si (a-Si) films are transparent for photons of which the energy is lower than a specific value, which is one of evidences that a-Si films are semiconductor.

The dependence of the optical absorption coefficient α of amorphous semiconductors on the photon energy $h\nu$ could be often represented by $\sqrt{\alpha h\nu} = B(h\nu - E_{opt})$, where B and E_{opt} are constants.[1] In the early stage of study on amorphous semiconductor, *Tauc* has discussed the relation and proposed that the E_{opt} in the relation could represent the band gap in amorphous semiconductors, where the E_{opt} is called by the optical gap energy.[2]

Optical absorption of a-Si and its alloys is an important subject in their applications, since a-Si and its alloys are promising photoconductive materials. Compared with the crystalline Si, a-Si shows stronger optical absorption, which could yield the effective solar-energy-conversion in thinner films than 1 μm.[3] Since one of important purposes of the nitrogen incorporation into a-Si is widening the optical gap,[4,5] it appears that the dependence of optical absorption on the nitrogen content is principal in characterizations of a-Si:N films.

In this chapter, the optical absorption, optical gap, and refractive index of CVD a-Si:N films are described, and their dependence on the incorporated nitrogen content is discussed.

4.2 EXPERIMENTS

The transmittance of films on fused quartz substrates was measured by a double beam spectrometer, and typical transmittance spectra at the visible and infrared regions are shown in Fig.4.1. The transmittance waves with respect to the wavelength longer than 1 μm, which could result from the interference among lightwaves multi-reflected between air-film and film-substrate interfaces. The transmittance of specimens, T, could be represented by

$$T = \frac{(1-R_1)(1-R_2)(1-R_3)\exp(-\alpha d)}{1+R_1R_2\exp(-2\alpha d) - 2r_1r_2\exp(-\alpha d)\cos(4\pi nd/\lambda)}\ , \tag{4.1}$$

where

$$R_1=\left(\frac{n-1}{n+1}\right)^2,\ R_2=\left(\frac{n-n_s}{n+n_s}\right)^2,\ R_3=\left(\frac{n_s-1}{n_s+1}\right)^2,\ r_1=\frac{1-n}{1+n}\ ,\ \text{and}\ r_2=\frac{n_s-n}{n_s+n}\ .$$

Here, n and n_s denote the refractive indices of a film and a substrate, α the absorption coefficient, d the film thickness, and λ the wavelength, respectively. n_s is 1.46 for the fused quartz used in this study. In the derivation of Eq.(4.1), the multiple reflections between film-substrate and substrate-air interfaces or between air-film and substrate-air interfaces could be neglected, since $R_2R_3 \leqq 6\times10^{-3}$ and $R_1(1-R_2)R_3 \leqq 9\times10^{-3}$ in this study. When the absorption coefficient α is so small that $\exp(-\alpha d) \cong 1$, from Eq.(4.1) the maximum or minimum transmittance, T_{max} or T_{min}, is equal to

$$T_{max} = \frac{16n_s^2}{(n_s+1)^4} \qquad \text{at}\ \lambda=\frac{2nd}{m}\ , \tag{4.2}$$

or

$$T_{min} = \frac{16\,n^2n_s^2}{(n_s^2+1)^2(n^2+n_s)^2} \qquad \text{at}\ \lambda=\frac{4nd}{2m+1}\ , \tag{4.3}$$

where m is the integer. As shown in Fig.4.1, the maximum transmittance at $\lambda = 1.78$ μm is 0.93, which agrees with the maximum transmittance obtained by Eq.(4.2) with $n_s = 1.46$. Therefore, it is considered that the optical absorption is so small that $\exp(-\alpha d) \cong 1$ beyond 1.78 μm. Then, the refractive index of a film could be evaluated

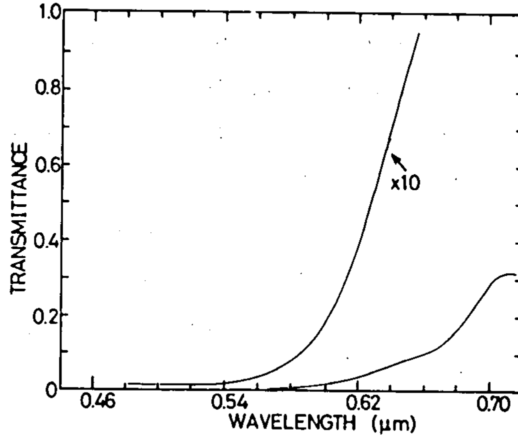

(a)

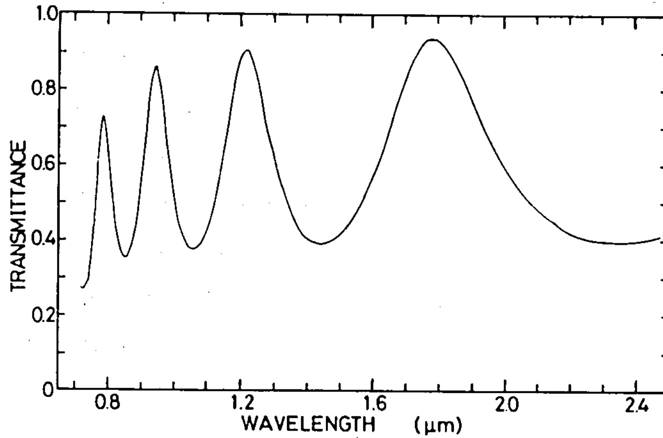

(b)

FIGURE 4.1 Typical transmittance spectra of a CVD a-Si:N film at visible (a) and infrared (b) light.

from the minimum transmittance at $\lambda = 2.35$ µm in Fig.4.1 by Eq.(4.3). Further, the film thickness d could be also obtained by

$$d = \frac{1}{4n} / \left(\frac{1}{\lambda_1} - \frac{1}{\lambda_2} \right) , \tag{4.4}$$

where λ_1 is the wavelength at the minimum (maximum) transmittance and λ_2 is the wavelength at the maximum (minimum) transmittance

adjacent to λ_1 ($\lambda_1 < \lambda_2$).

The optical absorption coefficient α could be evaluated from the transmittance T by Eq.(4.1). It is noted that the denominator of Eq.(4.1) is approximately equal to unity in the strong absorption region of $\exp(-\alpha d) \leq 0.3$, at which the multiple reflection could be neglected. This approximation is reasonable for results below $\lambda =$ 0.66 μm in Fig.4.1. The absorption coefficient beyond 0.66 μm could be evaluated from the maximum or minimum transmittance by substituting $\cos(4\pi nd/\lambda) = \pm 1$ into Eq.(4.1).

4.3 OPTICAL ABSORPTION AND OPTICAL GAP

Figure 4.2 shows the optical absorption coefficient of CVD a-Si:N films evaluated from transmittance measurements. In the figure, results on the absorption coefficient of a GD a-Si:H film were evaluated from the photo-acoustic spectroscopy and transmittance measurement by Yamasaki *et al.*[6] The optical gaps of CVD a-Si:N films are 1.5 eV, 1.55 eV, and 1.7 eV at the mole fraction of nitrogen atoms to silicon atoms, x, of 0, 0.2, and 0.4, respectively. As shown in the figure, the nitrogen incorporation decreases the optical absorption coefficient. The decrease in the optical absorption coefficient is more remarkable above the optical gap than below it. It could be considered that the optical absorption above the optical gap originates from the band-to-band excitation, while below it from the excitation from and/or to the gap states. Compared with GD a-Si:H films, CVD a-Si:N films show stronger absorption below the optical gap. Thus, CVD a-Si:N films would contain more gap states than GD a-Si:H films.

Figure 4.3 shows typical absorption spectra of CVD a-Si:N films plotted for $\sqrt{\alpha h\nu}$. The optical gap is obtained from the intercepts. Figure 4.4 shows the optical gap of films containing various amounts of nitrogen atoms. The optical gap of a-Si_3N_4 prepared at 1000°C is 5.3 eV.[7] The optical gap of films containing nitrogen atoms up to 2×10^{22} cm^{-3} ($x \simeq 0.4$) did not increase drastically. It was reported

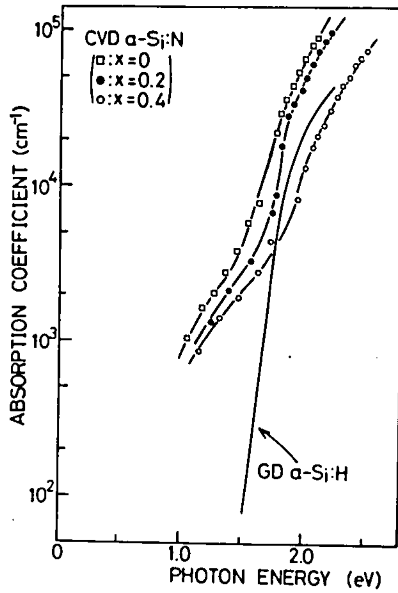

FIGURE 4.2 Optical absorption coefficient of CVD a-Si:N films containing various amounts of nitrogen atoms and a GD a-Si:H film.

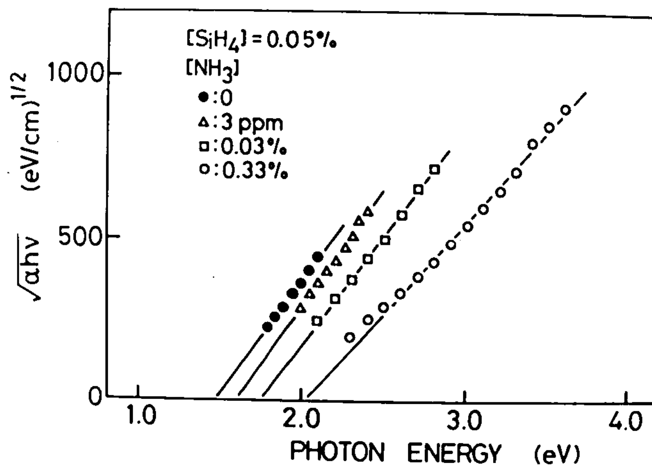

FIGURE 4.3 $\sqrt{\alpha h\nu}$ vs. $h\nu$ plots of absorption coefficient of CVD a-Si:N films.

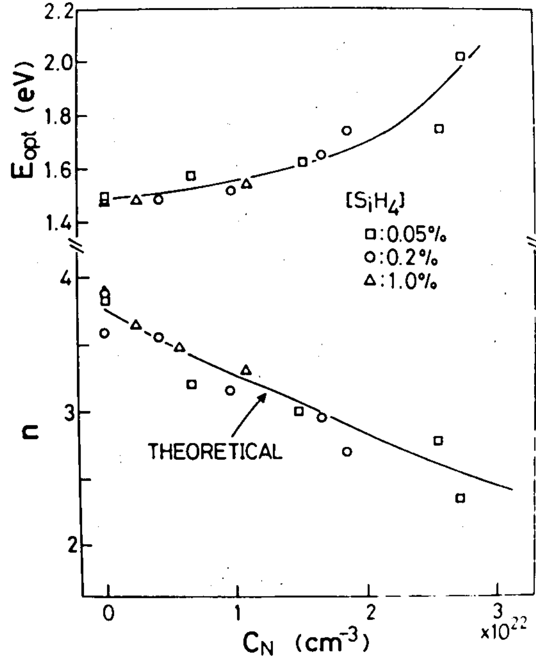

FIGURE 4.4 Optical gap E_{opt} and refractive index n of CVD a-Si:N films containing various amount of nitrogen atoms.

on GD a-Si:N films that the optical gap increased greatly beyond the mole fraction of nitrogen atoms to silicon atoms, $x = 1$. It is known that the energy gaps in crystalline semiconductor alloys are often approximated by a quadratic dependence on composition, *i.e.*,

$$E_{g(y)} = E_1 + (E_2 - E_1)y + c(y^2 - y) \quad , \tag{4.5}$$

where y and c are the composition and the bowing factor, respectively. With the assumption that the optical gap variation in amorphous semiconductors is similar to that in crystalline semiconductors, from the results shown in Fig.4.4, the bowing factor in a-Si:N films, for which the composition y is derived from the mole fraction x by $y = 3x/4$, can be evaluated as 3.5 eV.

4.4 REFRACTIVE INDEX

Figure 4.4 also shows the refractive index of films containing various amounts of nitrogen. The refractive index varies monotonically with the nitrogen content. It is well known that the refractive index is equal to the square root of the dielectric constant resulting from electronic polarization of substance atoms. The dependence of the dielectric constant of a-SiN_x on the mole fraction of nitrogen atoms to silicon atoms, x, was deduced by Phillip[7] as

$$\varepsilon = \left(1 - \frac{3}{4}x\right)^2 \varepsilon_{a\text{-}Si} + \frac{3}{4}x\, \varepsilon_{a\text{-}Si_3N_4} , \qquad (4.6)$$

in which nitrogen atoms were assumed to be incorporated homogeneously. Here, $\varepsilon_{a\text{-}Si}$ and $\varepsilon_{a\text{-}Si_3N_4}$ are the dielectric constants of a-Si and a-Si_3N_4, respectively. The refractive index evaluated from Eqs.(3.6) and (4.6) and $n = \sqrt{\varepsilon}$ is shown in Fig.4.4. The calculated values agree with the experimental ones. Therefore, it might be possible to evaluate the incorporated nitrogen content in an a-Si:N film from its refractive index.

4.5 SUMMARY

Optical absorption, optical gap, and refractive index of CVD a-Si:N films have been evaluated from their transmittance spectra and discussed. These results can be summarized as follows.

(i) The optical gap is increased from 1.5 to 2.0 eV by the nitrogen incorporation up to 2.8×10^{22} cm^{-3}. The dependence of the optical gap on the mole fraction of nitrogen atoms to silicon atoms, x, is approximated by

$$E_{opt} = 1.5 + 3.5\left(\frac{3}{4}x\right)^2 \quad (eV).$$

(ii) The nitrogen incorporation decreases the optical absorption coefficient. The optical absorption coefficient above the optical gap is more decreased by the nitrogen incorporation than below it.

Compared with glow-discharge deposited a-Si:H, CVD films show stronger optical absorption below the optical gap.

(iii) The refractive index is decreased from 3.5 to 2.2 by the nitrogen incorporation up to 2.8×10^{22} cm^{-3}. The dependence of the refractive index on the mole fraction of nitrogen atoms to silicon atoms could be explained by a model proposed by Phillip.

REFERENCES

1) N.F. Mott and E.A. Davis, *Electronic Processes in Non-Crystalline Materials, 2nd ed.*, (Clarendon, Oxford, 1979), p.290.
2) J. Tauc and A. Menth, J. Non-Cryst. Solids, 8-10 (1972) 569.
3) Y. Hamakawa, Solar Energy Materials, 8 (1982) 101.
4) D.A. Anderson and W.E. Spear, Philos. Mag., 35 (1977) 1.
5) H. Kurata, M. Hirose, and Y. Osaka, Jpn. J. Appl. Phys., 20 (1981) L811.
6) S. Yamasaki, H. Okushi, A. Matsuda, H. Oheda, N. Hata, and K. Tanaka, Jpn. J. Appl. Phys., 20 (1981) L665.
7) H.R. Phillip, J. Electrochem. Soc., 120 (1973) 295.

V. ELECTRICAL PROPERTIES OF CHEMICALLY VAPOR-DEPOSITED AMORPHOUS SILICON-NITROGEN ALLOYS

5.1 INTRODUCTION

It has been considered that the carrier transport in amorphous semiconductors is based on the extended-states conduction and the hopping conduction[1]. It could be understood that the extended-states conduction is similar to the band conduction in crystalline semiconductors. The dark conductivity originated by the extended-states conduction is often represented by[1] $\sigma = \sigma_0 \exp(-\Delta E/k_B T)$, where σ_0 is called by the minimum metallic conductivity and ΔE is considered to equal the energy difference between the mobility edge and the Fermi level, since carriers would be thermally activated from the gap states just below the Fermi level into the extended states. The hopping conduction is due to hopping of carriers through the gap states and could often dominate the carrier transport around room temperature in non-hydrogenated a-Si. It is reported that the dark conductivity originated by the hopping conduction is strictly related to the number of defects evaluated by the electron spin resonance[2].

It is considered that carriers could be excited into the extended states by photon irradiation which would increase the conductance. These increases in the conductance by photon irradiation could be strongly influenced by the gap states at which the photo-excited carriers recombine.

In this chapter, electric transport properties of CVD a-Si:N films are described and discussed. The nitrogen incorporation decreases the hopping conduction, which could be understood by decreases in gap states. The increase in conductance by photon irradiation is little influenced by the nitrogen incorporation.

5.2 DARK CONDUCTIVITY

The dark conductivity of films was measured in a coplanar structure with aluminum electrodes at an applied electric field of 400 ∿

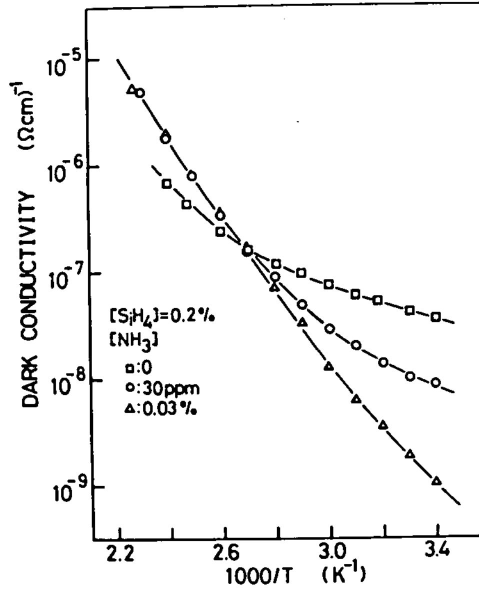

FIGURE 5.1 Typical temperature dependence of dark conductivity of CVD a-Si:N films deposited at 550°C.

800 V/cm. Figure 5.1 shows typical temperature dependence of the dark conductivity of a-Si:N films prepared at the silane gas concentration of 0.2% and 550°C. The temperature dependence of dark conductivity of films are well approximated by

$$\sigma = \sigma_1 \exp\left(-\frac{E_1}{k_B T}\right) + \sigma_2 \exp\left(-\frac{E_2}{k_B T}\right) , \tag{5.1}$$

where $E_1 > E_2$. A similar dependence was also reported on CVD a-Si[3] and evaporated a-Si.[4] The values of the preexponential factor and activation energy are shown in Fig.5.2. For the films deposited at large NH_3-gas concentrations, the second term in the equation is small relative to the first term and increases the dark conductivity slightly from the values of the first term near room temperature. Thus, σ_2 and E_2 are not included in the evaluation for these films. The values of E_1 are close to half of the optical gap, and σ_1 is close to the minimum metallic conductivity which is deduced to be $100 \sim 600$ $(\Omega\mathrm{cm})^{-1}$.[1] Therefore, the first term in Eq.(5.1) is consid-

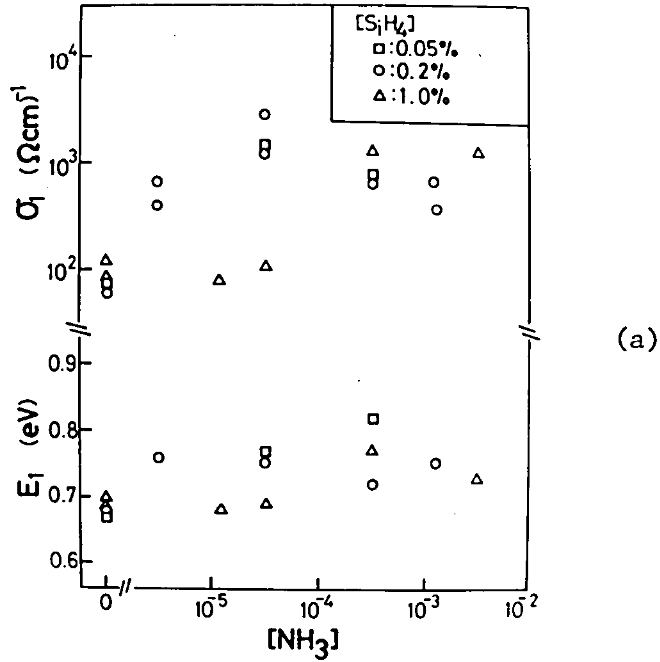

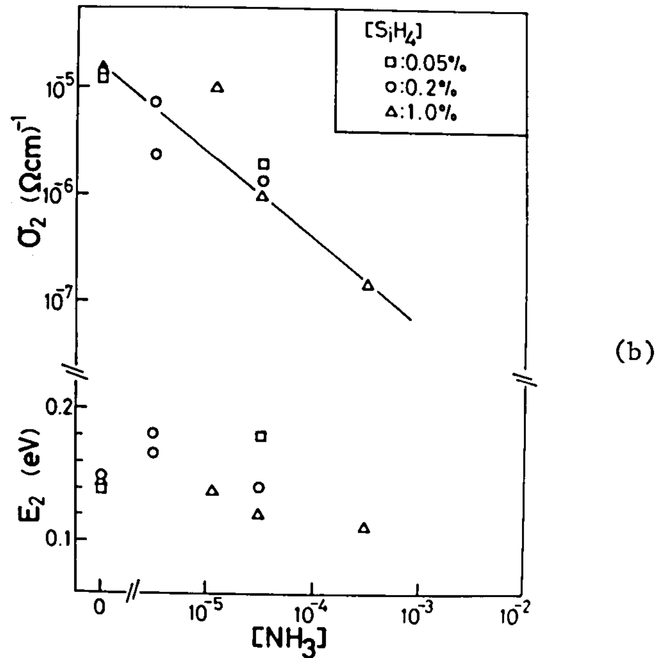

FIGURE 5.2 Preexponential factors and activation energies in temperature dependence of dark conductivity of CVD a-Si:N films.

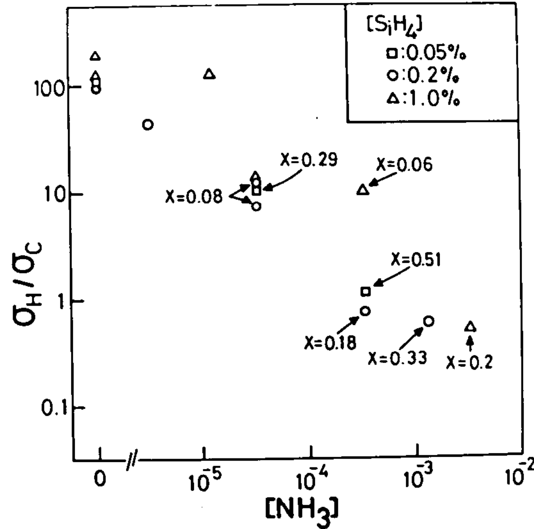

FIGURE 5.3 Reduction of hopping conduction by nitrogen incorporation. σ_H and σ_C denote conductivity at 300 K due to hopping conduction and extended-states conduction, respectively.

ered to be related to carrier transport in the extended states. On the other hand, the second term is considered to be due to the hopping conduction through the gap states.[1] The activation energy of $0.1 \sim 0.2$ eV in hopping conduction was reported on CVD a-Si[3,5] and evaporated a-Si.[4] Besides, it was reported that the activation energy implies a rapid increase in gap-state density about $0.1 \sim 0.2$ eV above the Fermi level.[4] The interpretation of the preexponential factor of hopping conduction is not well established at this stage. However, the conductivity due to hopping conduction is closely related to the gap-state density around the Fermi level.

Figure 5.3 shows the ratio of hopping conduction to extended-states conduction at 300 K. In the figure, x denotes the mole fraction of nitrogen atoms to silicon atoms. As shown in the figure, the hopping conduction is reduced by the nitrogen incorporation at any silane gas concentration. Therefore, it can be considered that the gap-state density around the Fermi level is reduced by the nitrogen

incorporation. In the next chapter, it is described that the nitrogen incorporation decreases the number of paramagnetic defects and the gap-state density evaluated by the field-effect method.

5.3 PHOTORESPONSE

Figure 5.4 shows the spectral photoresponse of 0.6-μm-thick CVD a-Si:N films, which is flat for incident photons of which the energy is 2.3∿2.8 eV as shown in the figure. The increase in the conductance by photon irradiation, ΔG, is related to the mobility μ and lifetime τ of photo-excited excess carriers, *i.e.*

$$\Delta G = \frac{W}{L} q I_0 (1 - R)\{1 - \exp(-\alpha d)\}\eta\mu\tau \quad , \tag{5.2}$$

where L (cm) and W (cm) are the gap and width of the electrodes, I_0 (photons/cm^{2}s) the flux of incident photons, R, α (cm^{-1}), and η are the reflectivity, absorption coefficient, and quantum efficiency, respectively. As described in Chapter IV, the absorption coefficient decreases rapidly with decreases of the photon energy, which yields the rapid decrease in ΔG with decreases of the photon energy from

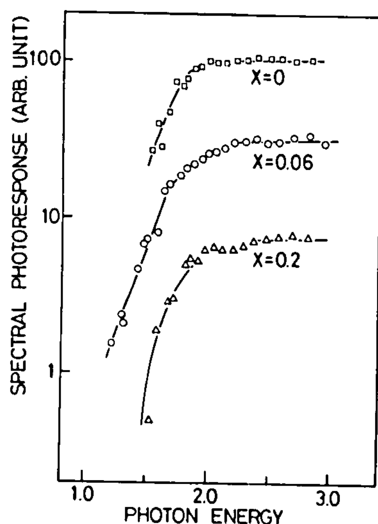

FIGURE 5.4 Spectral photoresponse of CVD a-Si:N films.

Eq.(5.2). The flat response of ΔG in the range of 2.3∿2.8 eV could be understood by $\alpha d > 1$ and constant $\eta\mu\tau$ product in this range. The non-linear dependence between ΔG and I_0 was reported on GD a-Si:H[6], which could be explained by that the recombination lifetime τ depends on I_0. However, ΔG of CVD a-Si:N films was proportional to I_0.

Figure 5.5 shows the $\eta\mu\tau$ product of CVD a-Si:N films at 300 K, which is little varied by the nitrogen incorporation. Although the recombination lifetime of photo-excited excess carriers into the extended states could be associated with the number of recombination centers, it has been proposed on the photoresponse of CVD a-Si that the conduction of carriers due to hopping might be enhanced by photon irradiation[3]. As shown in Fig.5.3, the hopping conduction dominates the conductivity around room temperature in CVD a-Si:N films including a few nitrogen atoms. Therefore, the increase in the conductance in these films might result from increases in the number of hopping carriers and might be independent of the number of recombination centers. Further, contradictory results[7,8] were reported on relationship between ΔG and the gap-state density near the Fermi level, which appears to result from complicated recombination process due to continuous distribution of gap states. Therefore, it has not been

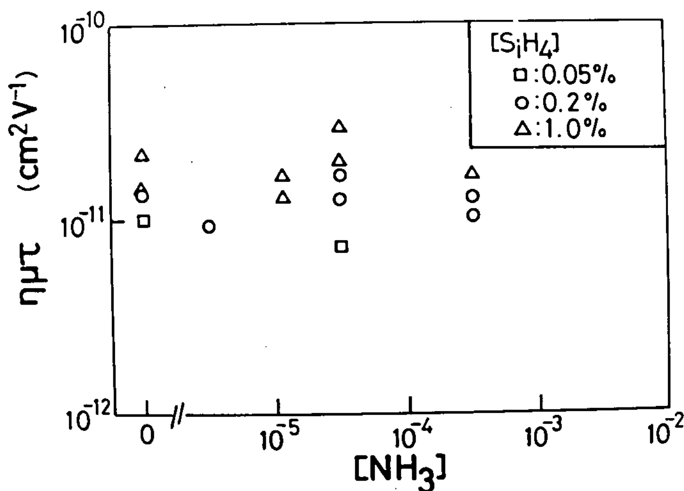

FIGURE 5.5 Product of quantum efficiency, mobility, and lifetime.

concluded whether the nitrogen incorporation influences the recombination centers in CVD a-Si.

5.4 SUMMARY

The dark conductivity and the photoresponse of CVD a-Si:N films have been described and discussed. The results can be summarized as follows.

(i) The nitrogen incorporation reduces the hopping conduction, which would be due to decreases of the gap-state density.

(ii) The activation energy of the extended-states conduction in films is from 0.7 to 0.8 eV, which would suggest that the Fermi level locates around the midgap.

(iii) The photoresponse of films is the order of 10^{-11} cm^2/V and little dependent on the nitrogen content.

It is considered that these electrical properties are dominated by the defects or gap states. In the next chapter, it is shown that the number of paramagnetic defects and the gap-state density evaluated by the field-effect method could be decreased by the nitrogen incorporation. Thus, decreases of the hopping conduction by the nitrogen incorporation could be well understood by decreases in the gap states around the Fermi level.

REFERENCES

1) N.F. Mott and E.A. Davis, *Electronic Processes in Non-Crystalline Materials* (Clarendon, Oxford, 1979) chapter 6.
2) T. Shimizu, M. Kumeda, and S. Ueda, Oyo Buturi, 50 (1981) 1266 (*in Japanese*).
3) M. Hirose, M. Taniguchi, and Y. Osaka, *Proc. 7th Int. Conf. on Amorphous & Liquid Semiconductors, Edinburgh, 1977* (Center for Industrial Consultancy and Liaison, University of Edinburgh,1977) p.352.
4) T. Nakashita, M. Hirose, and Y. Osaka, Jpn. J. Appl. Phys., 17 (1978) 985.

5) T. Nakashita, M. Hirose, and Y. Osaka, Jpn. J. Appl. Phys., 20 (1981) 471.

6) D.A. Anderson and W.E. Spear, Philos. Mag., 36 (1977) 695.

7) D.A. Anderson, G. Moddel, R.W. Collins, and W. Paul, Solid State Commun., 31 (1979) 677.

8) T.D. Moustakas, C.R. Wronski, and T. Tiedje, Appl. Phys. Lett., 39 (1981) 721.

VI. DEFECTS AND GAP STATES IN CHEMICALLY VAPOR-DEPOSITED AMORPHOUS SILICON-NITROGEN ALLOYS

6.1 INTRODUCTION

Paramagnetic defects in amorphous Si (a-Si) can be detected by electron spin resonance (ESR). Chemically vapor-deposited (CVD) a-Si contains the paramagnetic defects of which the g-values are 2.0043, 2.0055, and 2.011.[1-3] The defects of $g = 2.0055$ are found in non-doped CVD a-Si films, $g = 2.0043$ in P-doped films, and $g = 2.011$ in B-doped films.[1-3] These defects have been supposed to be a neutral Si dangling bond for $g = 2.0055$, a negatively charged weak bond between Si atoms or a trapped electron by conduction band tail for 2.0043, and a positively charged weak bond or a trapped hole by valence band tail for 2.011.[1,2] Paramagnetic defects are also found in CVD Si_3N_4 films and are supposed to be Si dangling bonds.[4,5] Similar results have been reported on glow-discharge (GD) or sputter deposited SiN films.[6,7] The g-value and line width of these defects are monotonically varied with the nitrogen content, which could be understood by the interaction between Si dangling bond and nitrogen atoms.[7]

The results on dark conductivity of CVD a-Si:N films described in Chapter V suggested that the nitrogen incorporation into CVD a-Si decreases the gap-state density which would result from defects. In this chapter, the effects on nitrogen incorporation on defects and gap-state density are investigated by ESR and field-effect measurements.

6.2 ELECTRON SPIN RESONANCE (ESR)

Undoped CVD a-Si and a-$SiN_{0.2}$ films[22] were investigated by ESR measurements. Films were about 0.5 μm thick and deposited onto fused quartz substrates. The gas concentrations for a-$SiN_{0.2}$ film deposition were 1% of SiH_4 and 0.33% of NH_3. ESR measurements were performed in the microwave frequency of 9.439 GHz at room temperature. Figure 6.1 shows the ESR spectra of undoped a-Si and

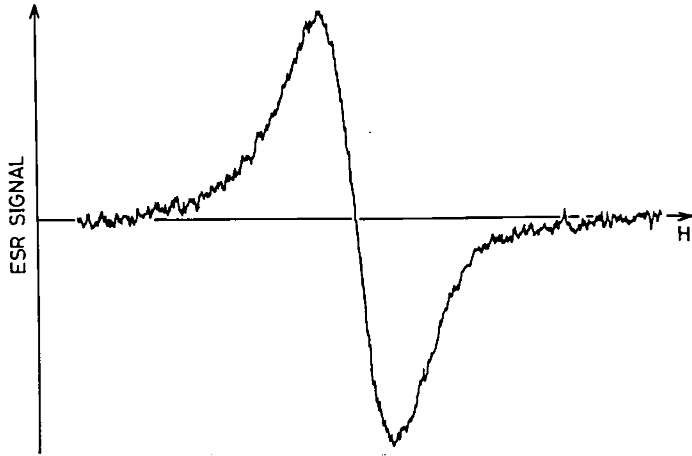

(a)

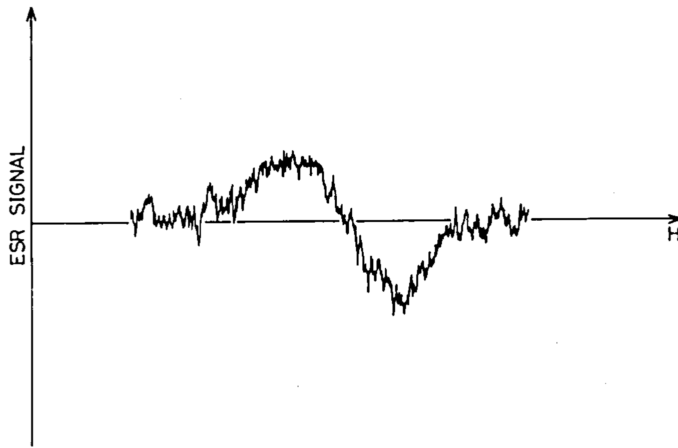

(b)

FIGURE 6.1 ESR spectra of CVD a-Si (a) and a-$SiN_{0.2}$ (b) films at room temperature. Their peak-to-peak line widths are 5.3 and 7.5 Gauss, respectively.

a-$SiN_{0.2}$ films. The g-value is 2.005. The ESR spectrum of localized electron around ^{14}N atoms is split into three resonant lines,[8] since the nuclear spin of ^{14}N is one. However, the ESR spectrum of a-$SiN_{0.2}$ showed a single resonant line. Therefore, dominant ESR centers in the a-$SiN_{0.2}$ film are considered to be localized around Si atoms similarly to the undoped a-Si film. These ESR centers would

originate from Si dangling bonds. It has been reported that the ESR signal due to the nitrogen defects is neither observed in GD a-Si:N:H[6] sputter deposited a-Si:N[7] and CVD Si_3N_4.[4,5] It has been proposed that the N dangling bonds in a-Si:N films could be spinless due to valence alternation pairs[7,9] although the contrary has been proposed.[21]

The relative spin density of CVD a-$SiN_{0.2}$ to that of undoped a-Si which is evaluated from their ESR spectra is one-fifth, which would suggest that the number of Si dangling bonds in CVD a-Si is reduced by the nitrogen incorporation. It is understood that the hydrogen incorporation into a-Si drastically reduces the number of Si dangling bonds.[2,10,11] Further, it has been reported that CVD a-Si could contain the hydrogen of which the concentration in films deposited at 550°C is about 0.7 at%.[12] Therefore, decreases of the dangling bonds by the nitrogen incorporation might be understood by increases of incorporated hydrogen atoms by it. Alternatively, the nitrogen incorporation into a-Si makes Si random networks more flexible.[7]

The peak-to-peak line widths in the ESR spectra of undoped CVD a-Si and a-$SiN_{0.2}$ films are 5.3 and 7.5 Gauss, respectively. It has been reported that the line width in the ESR spectrum from Si dangling bonds is broadened by the dangling bond-nitrogen interaction.[7] However, it has been reported that the line width in CVD a-Si or GD a-Si:H narrows with increases in the number of ESR centers,[3,14,15] which could be understood by the exchange narrowing due to *g*-factor anisotropy.[14,15] It could not been known at present whether the broadning of the line width in the ESR spectrum of CVD a-Si by the nitrogen incorporation is due to the dangling bond-nitrogen interaction or the reduction in the spin density.

6.3 GAP-STATE DENSITY EVALUATED BY FIELD-EFFECT METHOD

Field-effect measurements were carried out for the films deposited on thermally oxidized Si substrates. The substrates were n^+ crystalline Si substrates of which the resistivity is 0.003 Ωcm and used for a gate electrode. The thermally oxidized layer was 1100 Å

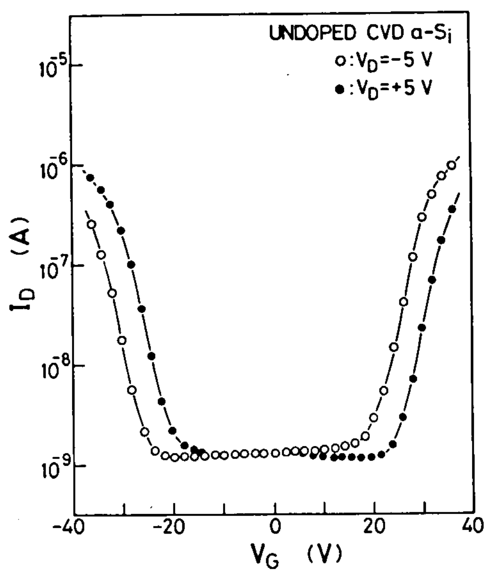

(a)

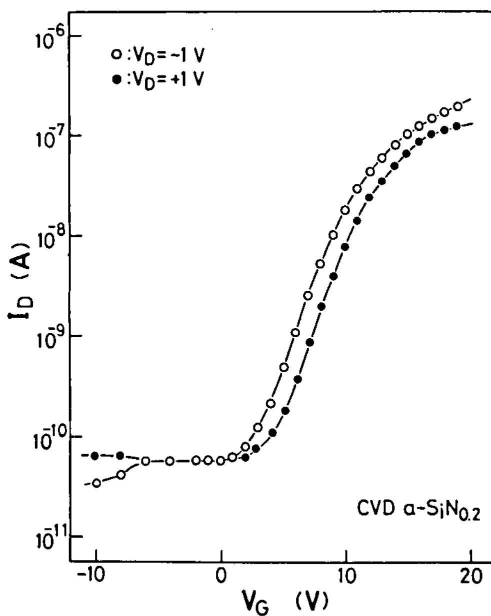

(b)

FIGURE 6.2 Field effect of undoped CVD a-Si film (a) and $a\text{-}SiN_{0.2}$ films (b) at room temperature.

thick. In the procedure, CVD a-Si or $SiN_{0.2}$ films were deposited subsequent to the oxidation of Si substrates in a reactor after eliminating oxygen in that reactor by a vacuum pump. Figure 6.2 shows the field effect of undoped and doped films at room temperature. The channel conductance of the undoped film is symmetric with respect to the gate voltage and little modulated by gate voltage lower than 20 volts. This U-shaped characteristic is considered due to the existance of large hopping conduction which could not be modulated by the gate voltage. Further, this would imply that the Fermi level is located near the mid-gap, and that the flat-band voltage is around 0 volts. On the other hand, the channel conductance of the doped film rises rapidly at positive gate-voltages. Therefore, the doped film is considered to be n-type.

Elevation of measurement temperature is preferable to derive the gap-state density in CVD a-Si by the field effect method. Thus, the gap-state density was evaluated from the results of the field effects at 84°C and 114°C for the undoped and doped films, respectively.

Figure 6.3 shows the derived gap-state density in undoped and doped films. It appears that the gap-state density at $0.1\ \text{eV} \leqq E - E_F \leqq 0.3\ \text{eV}$ is reduced by the nitrogen incorporation. This result agrees with the reduction of the hopping conduction in dark conductivity described in the previous chapter. As discussed in the previous section, the Si dangling bonds could be decreased by the nitrogen incorporation. Therefore, the gap states due to Si dangling bonds would be located at $E - E_F < 0.3$ eV. These states would be negatively charged Si dangling bond states. Similar results have been reported on GD a-Si:H.[16-20] On the other hand, it seems that the nitrogen incorporation increases the gap-state density around $E - E_F = 0.4$ eV, which might be due to the creation of a new type of defect with it.

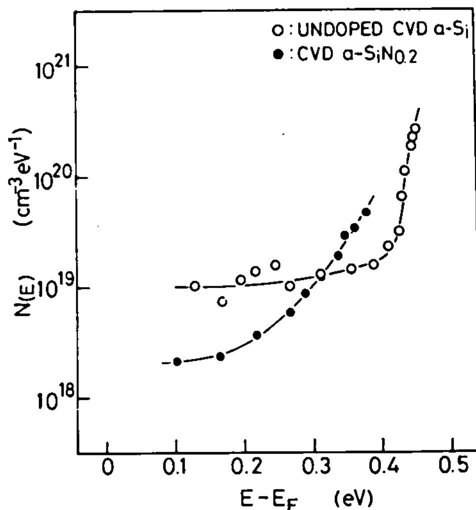

FIGURE 6.3 Gap-state densities in CVD a-Si and a-$SiN_{0.2}$ films evaluated by the field effect method.

6.4 SUMMARY

The effects of the nitrogen incorporation on defects and gap states in CVD a-Si have been investigated by ESR measurements and field effect method. Their results can be summarized as follows.

(i) Paramagnetic defects in CVD a-Si and a-$SiN_{0.2}$ films detected by ESR have the g-value of 2.005. The nitrogen incorporation into CVD a-Si decreases the number of these defects to one-fifth and increases the line width of the ESR spectrum.

(ii) The gap-state density at $0.1\ \text{eV} \leqq E - E_F \leqq 0.3\ \text{eV}$ evaluated by the field effect method was decreased by the nitrogen incorporation, which agrees with the results on dark conductivity described in Chapter V.

These reductions in the number of paramagnetic defects and the gap-state density could result from increases of the incorporated hydrogen atoms or structural relaxation. It is known that the incorporated hydrogen atoms in a-Si:H could be effused by thermal annealing. In the next chapter, effects of thermal annealing of CVD a-Si and a-$SiN_{0.2}$ films on their electrical properties, defects, and gap states are investigated with respect to the role of incorporated hydrogen.

REFERENCES

1) S. Hasegawa, T. Kasajima, and T. Shimizu, Philos. Mag., B43 (1979) 149.
2) J. Magarino, D. Kaplan, A. Friederich, and A. Denuville, Philos. Mag., B45 (1982) 285.
3) S. Hasegawa, T. Kasajima, and T. Shimizu, Solid State Commun., 29 (1979) 13.
4) S. Fujita, H. Toyoshima, M. Nishihara, and A. Sasaki, J. Elecron. Mater., 11 (1982) 795.
5) S. Fujita, H. Sato, and A. Sasaki, *The 163rd Meeting of Electrochemical Society (1983), San Fransisco.*
6) S. Yokoyama, M. Hirose, and Y. Osaka, Jpn. J. Appl. Phys., 20 (1981) L35.
7) T. Shimizu, S. Oozora, A. Morimoto, M. Kumeda, and N. Ishii, Solar Energy Materials, 8 (1982) 311.
8) K.L. Brower, Phys. Rev. Lett., 24 (1980) 1627.
9) C.T. Kirk, Jr., J. Appl. Phys., 50 (1979) 4190.
10) D. Kaplan, N. Sol, G. Velosco, and P.A. Thomas, Appl. Phys. Lett., 33 (1978) 440.
11) N. Sol, D. Kaplan, D. Dienmergard, and D. Deneuville, J. Non-Cryst. Solids, 35-36 (1980) 291.
12) D.C. Booth, D.D. Allred, and B.O. Seraphin, Solar Energy Materials, 2 (1979) 107.
13) M. Kumeda, S. Oozora, N. Ishii, A. Morimoto, and T. Shimizu, IECE Japan Rept. Tech. Group Electron Devices, ED82-65 (1982) 9 (*in Japanese*).
14) S. Hasegawa and Y. Imai, Philos. Mag., B45 (1982) 347.
15) U. Voget-Grote, W. Kummerle, R. Fischer, and J. Stuke, Philos. Mag., B41 (1980) 127.
16) K. Morigaki, Y. Sano, and I. Hirabayashi, Solid State Commun., 39 (1981) 947.
17) K. Morigaki, Y. Sano, and I. Hirabayashi, J. Phys. Soc. Japan, 51 (1982) 147.

18) N. Ishii, M. Kumeda, and T. Shimizu, Jpn. J. Appl. Phys., 21 (1981) L673.

19) H. Derch, J. Stuke, and J. Beicher, Phys. Stat. Solidi, (b)105 (1981) 265.

20) W.B. Jackson, Solid State Commun., 44 (1982) 477.

21) J. Robertson, Philos. Mag., B44 (1981) 215.

22) *The optical gap of films is 1.5 eV and 1.6 eV, respectively.*

VII. THERMAL ANNEALING OF CHEMICALLY VAPOR-DEPOSITED AMORPHOUS SILICON-NITROGEN ALLOYS

7.1 INTRODUCTION

Properties of hydrogenated amorphous Si (a-Si) are drastically varied by thermal annealing.[1-6] It has been reported that thermal annealing of glow-discharge (GD) deposited a-Si:H films above 300°C decreases the photoconductivity and the photoluminescence intensity.[3,4,6] It has been understood that these variations are associated with increases of defects which are supposed to be Si dangling bonds.[3,4,6] On the other hand, it was found that the incorporated hydrogen atoms are effused by thermal annealing.[1-3,5-8]

Since chemically vapor-deposited (CVD) a-Si are usually grown from SiH_4 at temperature above 500°C, the amount of incorporated hydrogen in the films at 550°C is about 0.7 at.%[9] and small as compared with that of GD a-Si:H films. The CVD a-Si contains many paramagnetic defects in a film[10-13] and shows large hopping conduction and poor photoconductivity, which has been supposed to result from few incorporated hydrogen atoms. In Chapters V and VI, it has been demonstrated that the nitrogen incorporation into CVD a-Si decreases the number of paramagnetic defects and the gap-state density. These decreases might result from increases of incorporated hydrogen atoms by the nitrogen incorporation. The contribution of incorporated hydrogen atoms to properties of CVD a-Si and a-Si:N films could be investigated by variations of their properties due to thermal annealing.

In this chapter, effects of thermal annealing which effuses the incorporated hydrogen atoms on the dark conductivity, paramagnetic defects, and gap-state density of CVD a-Si and a-Si:N films are described. Their results suggest that the defects and gap states in CVD a-Si and a-Si:N films could be reduced by the incorporated hydrogen, and the nitrogen incorporation relaxes the internal strain without breaking the bonds.

7.2 THERMAL ANNEALING

0.6-μm-thick undoped CVD a-Si and a-$SiN_{0.2}$ films[15] were thermally annealed in Ar flow at 550°C for 2 or 20 h. Here, the a-$SiN_{0.2}$ films were deposited at SiH_4 and NH_3 gas concentrations of 1% and 0.33%, respectively. It was confirmed by X-ray diffraction that 20-h annealed films were not crystallized. It is reported that CVD or evaporated a-Si is not crystallized by 100-h thermal annealing at 550°C[9,14] and nitrogen doping into a-Si restrains from the crystallization.[9] However, the structural change in a random network might be caused by the thermal annealing. The refractive index and thickness of the film were little decreased by it.

7.3 ELECTRON SPIN RESONANCE (ESR)

Figure 7.1 shows the ESR spectrum of a 20-h annealed CVD a-$SiN_{0.2}$ film. Since the spectrum is a single resonant line similar to that of the as-deposited film described in Chapter VI, the dominant paramagnetic defects in the annealed films would be also Si dangling bonds. Table 7.1 shows changes in the relative spin density derived from ESR spectra and the peak-to-peak line width of spectra by thermal annealing of undoped a-Si and a-$SiN_{0.2}$ films. Thermal annealing increases

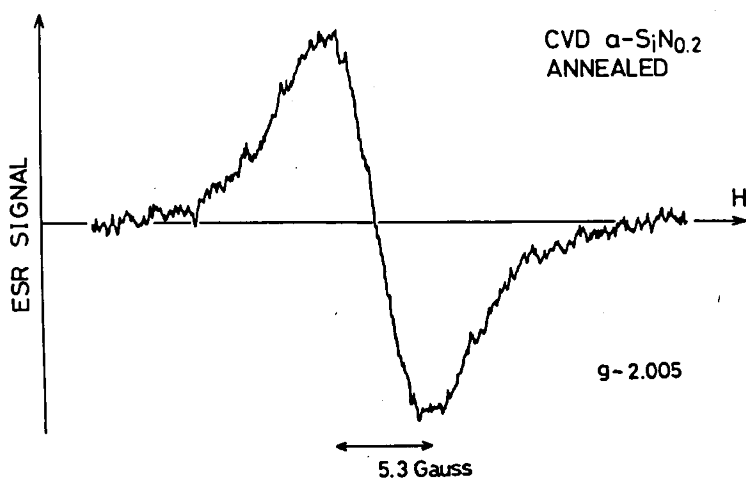

FIGURE 7.1 ESR spectrum of a 20-h annealed a-$SiN_{0.2}$ film.

TABLE 7.1 Relative spin density (upper) and line width (lower) of CVD a-Si and a-$SiN_{0.2}$ films.

	AS-DEPOSITED	ANNEALED
UNDOPED a-Si	5.0 5.3G	10 4.1G
a-$SiN_{0.2}$	1 7.5G	5.2 5.3G

the spin density both in undoped a-Si and a-$SiN_{0.2}$ films, which would result from the hydrogen effusion by it. It is noted that the increment of spin density in CVD a-$SiN_{0.2}$ films by thermal annealing is close to that in undoped a-Si films. If the hydrogen atoms in films were completely effused by 20-h annealing at 550°C, this suggests that the number of incorporated hydrogen atoms is close in undoped a-Si and a-$SiN_{0.2}$ films. Further, the spin density in the annealed a-$SiN_{0.2}$ film is smaller than that in the annealed a-Si film. Provided complete hydrogen effusion of films by 20-h thermal annealing at 550°C, it could be speculated that the nitrogen incorporation into a-Si decreases the number of Si dangling bonds due to structural changes in the network.

7.4 DARK CONDUCTIVITY

Figure 7.2 shows the temperature dependence of dark conductivity of as-deposited and 20-h annealed films. As described in Chapter V, these results can be well fitted by the sum of two activation terms, which could result from the extended-states conduction and the hopping conduction. The values of preexponential factors and activation energies are summarized in Table 7.2, where σ_1 and E_1 would be associated with the extended-states conduction, and σ_2 and E_2 with the hopping conduction. Thermal annealing increases the dark conductivity of both a-Si and a-$SiN_{0.2}$ films around room temperature, which could result from increases of the hopping conduction. Thus, it is considered that the gap-state density near the Fermi level is

TABLE 7.2 Changes of dark conductivity and activation energy by 20-h thermal annealing at 550°C.

		σ_{RT} $(\Omega cm)^{-1}$	σ_1 $(\Omega cm)^{-1}$	E_1 (eV)	σ_2 $(\Omega cm)^{-1}$	E_2 (eV)
UNDOPED	AS-DEPOSITED	7×10^{-8}	90	0.70	2×10^{-5}	0.15
	ANNEALED	2×10^{-6}	80	0.67	6×10^{-3}	0.16
a-$SiN_{0.2}$	AS-DEPOSITED	1×10^{-9}	1300	0.73	----	----
	ANNEALED	4×10^{-8}	1400	0.75	6×10^{-5}	0.19

is increased by the thermal annealing. In the annealed films, a-$SiN_{0.2}$ shows the hopping conduction smaller than a-Si. Thus, it is considered that the gap-state density near the Fermi level in the annealed films is smaller in a-$SiN_{0.2}$ film than in a-Si film, similarly to in as-deposited films. It is noted that the changes in the hopping conduction agree with the results on the ESR centers.

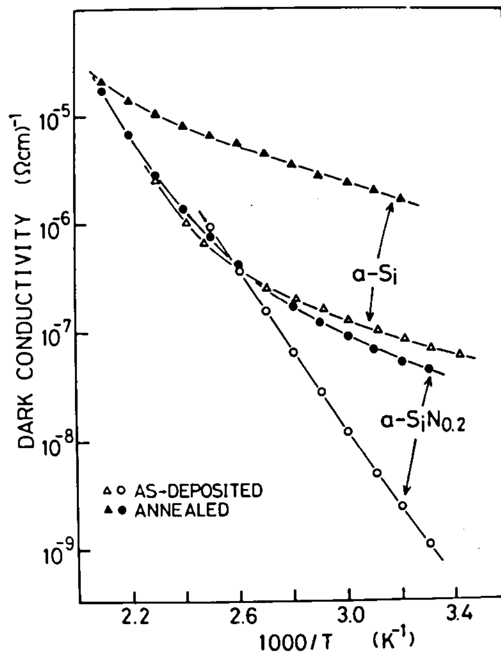

FIGURE 7.2 Temperature dependence of dark conductivity in as-deposited and 20-h annealed films.

7.5 GAP-STATE DENSITY EVALUATED BY FIELD-EFFECT METHOD

Figure 7.3 shows the field effect at room temperature of as-deposited and annealed a-$SiN_{0.2}$ films. The channel conductance in these films is strongly enhanced by positive gate voltage application. Since the elevation of measurement temperature is desired for the evaluation of gap-state density by the field-effect method, the field effect of films for the analysis of the gap-state density were measured around 100°C. Figure 7.4 shows the results on the field-effect gap-state density of as-deposited and annealed CVD a-$SiN_{0.2}$ films.

Although the gap-state density evaluated by the field-effect method might include the states at the interface between a-$SiN_{0.2}$ film and insulator, these results suggest that the gap-state density in CVD a-$SiN_{0.2}$ is increased about one order of the magnitude by 20-h thermal annealing. On the other hand, it is considered that the increase of the dangling bond states in bulk of a-$SiN_{0.2}$ films is a factor of five from the ESR measurement. This disagreement between the field-effect method and ESR measurement might be caused by that

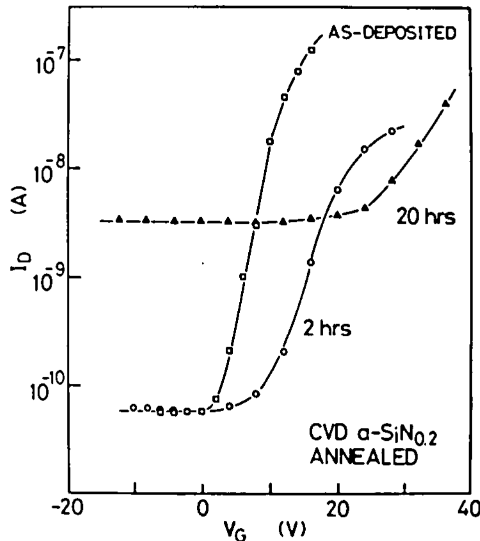

FIGURE 7.3 Field effects of as-deposited, 2-, and 20-h annealed a-$SiN_{0.2}$ films.

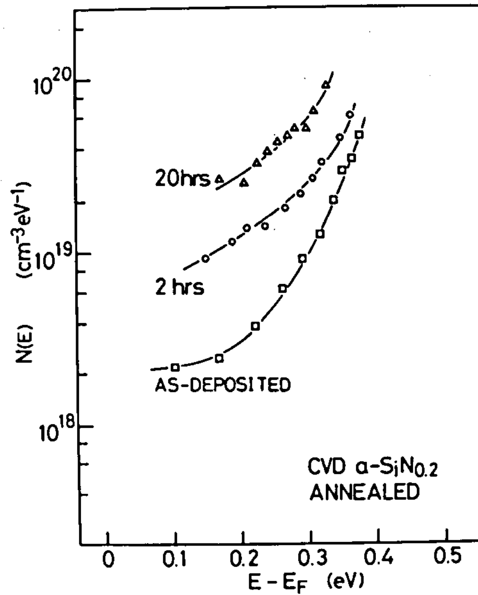

FIGURE 7.4 Field-effect gap-state density in as-deposited, 2-, and 20-h annealed a-$SiN_{0.2}$ films.

the hydrogen atoms effuse more drastically near the interface region than in the bulk. Alternatively, the thermal annealing might introduce the spinless defects into the CVD a-$SiN_{0.2}$ films or the interface states.

7.6 SUMMARY

Effects of thermal annealing on the paramagnetic defects, dark conductivity, and gap-state density by field-effect method of CVD a-Si and a-$SiN_{0.2}$ films have been investigated. Their results can be summarized as follows.

(i) The number of paramagnetic defects in CVD a-Si and a-$SiN_{0.2}$ films are increased by thermal annealing, which could be understood by that these films contain the bonded hydrogen atoms to Si atoms.

(ii) The nitrogen incorporation reduces the number of paramagnetic defects in thermally annealed a-Si films similarly to in as-deposited films. This suggests that the nitrogen incorporation relaxes the strain without breaking the bonds in a Si random network.

(iii) The hopping conduction in CVD a-Si and a-$SiN_{0.2}$ films is increased by thermal annealing, which could result from increases in the gap-state density near the Fermi level.

(iv) The field-effect measurements also showed the increase of the gap-state density by thermal annealing.

REFERENCES

1) J.I. Pankove and D.E. Carlson, Appl. Phys. Lett., 31 (1977) 450.
2) J.I. Pankove, Appl. Phys. Lett., 32 (1978) 812.
3) D.K. Biegelsen, R.A. Street, C.C. Tsai, and J.C. Knights, Phys. Rev. Lett., B20 (1979) 5238.
4) U. Voget-Grote, W. Kummerle, R. Fischer, and J. Stuke, Philos. Mag., B41 (1980) 127.
5) K. Zellama, P. Germain, S. Squelard, B. Bourdon, J. Frontille, and R. Danielon, Phys. Rev., B23 (1981) 6648.
6) S. Hasegawa and Y. Imai, Philos. Mag., B45 (1982) 347.
7) H. Fritzsche, M. Tanielian, C.C. Tsai, and P.J. Caczi, J. Appl. Phys., 50 (1979) 3366.
8) J.A. McMillan and E.M. Peterson, J. Appl. Phys., 50 (1979) 5238.
9) D.C. Booth, D.D. Allred, and B.O. Seraphin, Solar Energy Materials, 2 (1979) 107.
10) S. Hasegawa, T. Kasajima, and T. Shimizu, Solid State Commun., 29 (1979) 13.
11) M. Hirose, M. Taniguchi, T. Nakashita, Y. Osaka, T. Suzuki, S. Hasegawa, and T. Shimizu, J. Non-Cryst. Solids, 35-36 (1980) 297.
12) S. Hasegawa, T. Kasajima, and T. Shimizu, Philos. Mag., B43 (1981) 149.
13) J. Magarino, D. Kaplan, A. Friederich, and A. Denuville, Philos. Mag., B45 (1982) 285.
14) N.A. Blum and C. Feldman, J. Non-Cryst. Solids, 11 (1972) 242.
15) *The optical gap of films is 1.5 eV and 1.6 eV, respectively.*

VIII. POST-HYDROGENATION OF CHEMICALLY VAPOR-DEPOSITED AMORPHOUS SILICON-NITROGEN ALLOYS

8.1 INTRODUCTION

Defects and gap-state density in amorphous Si (a-Si) films could be decreased by the hydrogenation, which increases the photoconductivity.[1-5] Thus, various hydrogenation techniques of a-Si films during or after the deposition have been developed and improved.[1,2,6-16] The hydrogenation of a-Si films after the deposition (post-hydrogenation) could be achieved by annealing in H^+ plasma.[16-22,30]

In previous chapters, effects of the nitrogen incorporation on properties of chemically vapor-deposited (CVD) a-Si have been investigated. The nitrogen incorporation into CVD a-Si films changes the field effects from an intrinsic to n-type characteristic, although the activation energy in temperature dependence of the dark conductivity is not decreased. The photoconductivity of the as-deposited films is not increased by the nitrogen incorporation. On the other hand, it has been reported that the nitrogen incorporation into glow-discharge deposited (GD) a-Si:H films introduces donors and increases the photoconductivity.[23-27] Since the incorporated hydrogen atoms are fewer in CVD a-Si than GD a-Si, it could be considered that such differences in the effect of nitrogen incorporation on their electrical properties are due to differences in the incorporated hydrogen content.

In this chapter, properties of post-hydrogenated CVD a-Si:N films are described and discussed. It is shown that the activation energy in temperature dependence of dark conductivity of post-hydrogenated films is decreased by the nitrogen incorporation, and the photoconductivity of the films is increased by it similarly to results on GD a-Si:H films.

8.2 POST-HYDROGENATION

0.6-μm-thick undoped CVD a-Si and a-$SiN_{0.2}$ films[22] were post-

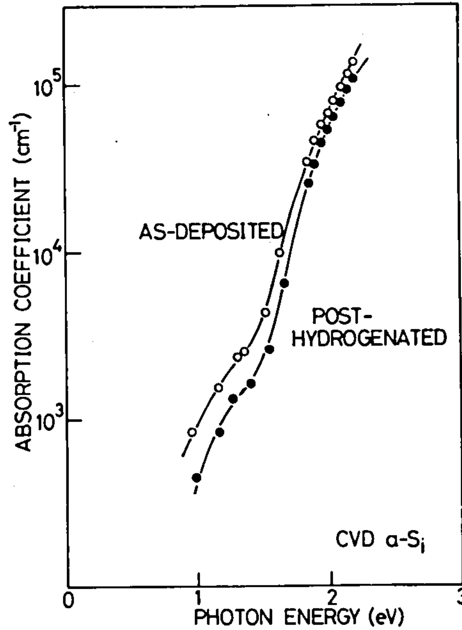

FIGURE 8.1 Absorption coefficient of as-deposited and post-hydrogenated CVD a-Si films.

hydrogenated in a capacitive coupling reactor in which the spacing and diameter of electrodes are 2 cm and 20 cm, respectively. Here, the SiH_4 and NH_3 concentrations at deposition of CVD a-$SiN_{0.2}$ films had been 0.2% and 0.03%, or 1% and 0.33%, respectively. The rf power and frequency at the post-hydrogenation were 300 W and 13.56 MHz. The post-hydrogenation of films were carried out at 5 Torr and 400°C for 1 h. Hydrogen plasma was turned off at the beginning of cooling down. The refractive index and thickness of the films were little changed by the post-hydrogenation, although the optical absorption coefficient was decreased by it as shown in Fig.8.1. Here, those were evaluated by assuming that films were homogeneous.

8.3 DARK CONDUCTIVITY

Figure 8.2 shows the temperature dependence of the dark conductivity in post-hydrogenated CVD a-Si and a-$SiN_{0.2}$ films. In an undoped CVD a-Si film, the hopping conduction disappears after post-

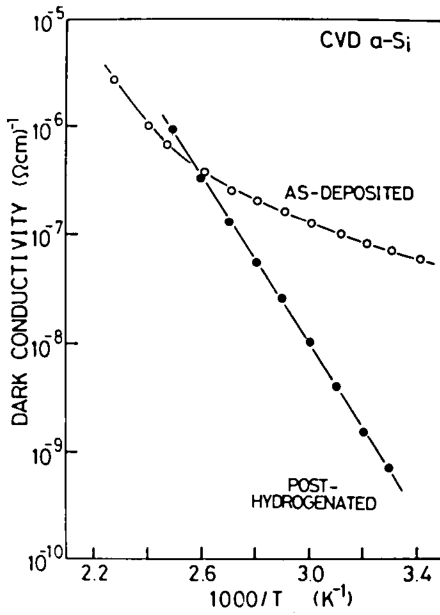

(a)

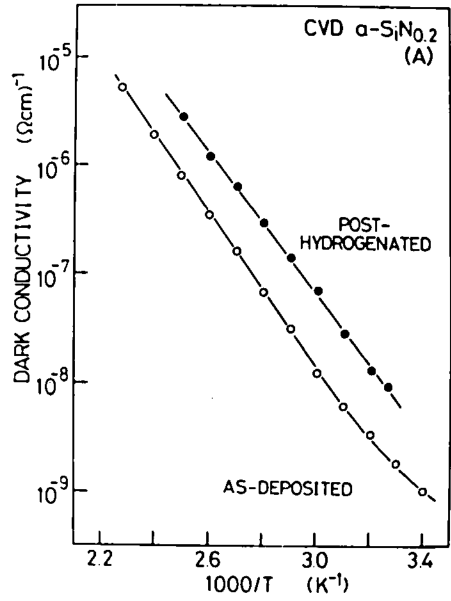

(b)

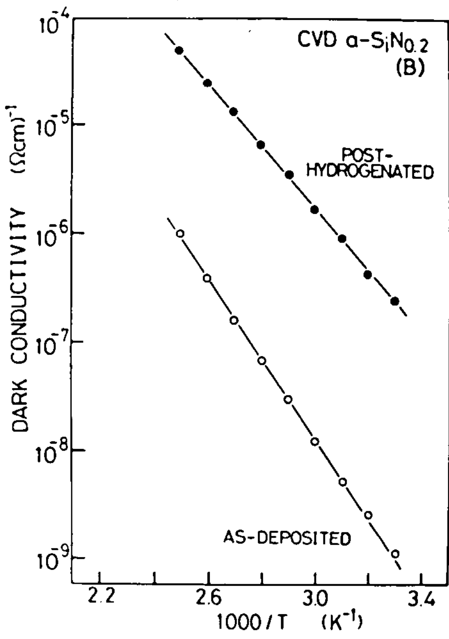

(c)

FIGURE 8.2

Temperature dependence of the dark conductivity of as-deposited and post-hydrogenated films. (a) undoped CVD a-Si, (b) a-$SiN_{0.2}$ at SiH_4 and NH_3 gases of 0.2% and 0.03%, and (c) a-$SiN_{0.2}$ at 1.0% and 0.33%, respectively.

TABLE 8.1 Post-hydrogenation effects on the dark conductivity and $\eta\mu\tau$ product of undoped CVD a-Si and a-$SiN_{0.2}$ films deposited at SiH_4 and NH_3 gas concentrations of 0.2% and 0.03% (A), and 1.0% and 0.33% (B), respectively.

		σ_{RT} $(\Omega cm)^{-1}$	σ_1 $(\Omega cm)^{-1}$	E_1 (eV)	$\eta\mu\tau$ (cm^2/V)
UNDOPED	AS-DEPOSITED	7×10^{-8}	90	0.70	2×10^{-11}
	POST-HYDROGENATED	7×10^{-10}	3000	0.76	4×10^{-9}
a-$SiN_{0.2}$	(A) AS-DEPOSITED	2×10^{-9}	700	0.71	2×10^{-11}
	POST-HYDROGENATED	8×10^{-9}	300	0.64	2×10^{-9}
	(B) AS-DEPOSITED	1×10^{-9}	1300	0.73	1×10^{-11}
	POST-HYDROGENATED	3×10^{-7}	1000	0.58	3×10^{-7}

hydrogenation. It can be considered that the gap-state density near the Fermi level is reduced by the post-hydrogenation. The activation energy is decreased by the post-hydrogenation in the a-$SiN_{0.2}$ films. The activation energies obtained from the results shown in Fig.8.2 are summarized in Table 8.1. It suggests the Fermi level shift towards the conduction band, since a-$SiN_{0.2}$ films are thought to be n-type from the field effect.

The Fermi level shift due to donor doping into a-Si, ΔE_F, is represented by[28]

$$N_D = \int_{E_F}^{E_F+\Delta E_F} N_{(E)} dE \,, \tag{8.1}$$

where N_D and E_F denote the concentration of ionized donors and the Fermi level, respectively. The Fermi level can be shifted towards the conduction band by decreasing the gap-state density around the Fermi level in the films containing ionized donors. Such Fermi level shift by post-hydrogenation was reported on phosphorus doped CVD a-Si films.[17,20] Therefore, the Fermi level shift in CVD a-$SiN_{0.2}$ by post-hydrogenation suggests that the films contain donors, since

the post-hydrogenation could decrease the gap-state density. When the gap-state density near the Fermi level in a post-hydrogenated a-$SiN_{0.2}$ film is assumed to be constant energetically and the order of 10^{17} $cm^{-3}eV^{-1}$, the concentration of ionized donors is deduced to be 10^{16} cm^{-3}.

8.4 PHOTOCONDUCTIVITY— PRODUCT OF QUANTUM EFFICIENCY, MOBILITY, AND LIFETIME

The product of quantum efficiency, mobility, and lifetime ($\eta\mu\tau$ product) for photoexcited excess carriers in post-hydrogenated CVD a-Si and a-$SiN_{0.2}$ films was evaluated from their photoresponse at the incident photon flux of 10^{17} photons/cm^2s and energy of 3 eV. The results are summarized in Table 8.1. The $\eta\mu\tau$ product of a film is increased by the post-hydrogenation similarly to previous works.[19,21,22] It was reported that the nitrogen incorporation into a-Si:H films enhances the photoconductivity.[25-27] The results shown in Table 8.1 suggest that the enhanced photoconductivity by the nitrogen incorporation does not depend on only the amount of incorporated nitrogen atoms, since the films prepared at the different conditions and containing the same amount of nitrogen atoms showed the different $\eta\mu\tau$ product by two orders of the magnitude. The photoconductivity might be enhanced by the Fermi level shift towards the conduction band, since it seems that the $\eta\mu\tau$ product is related to the activation energy of the dark conductivity. Similar results were also reported on electrical properties of phosphorus doped GD a-Si:H.[27]

8.5 SUMMARY

Properties of post-hydrogenated CVD a-Si:N films were measured and discussed. Their results can be summarized as follows.

(i) The activation energy in temperature dependence of the dark conductivity is little varied for undoped CVD a-Si films and decreased for a-Si:N films by the post-hydrogenation, which would be understood by the introduction of donors due to the nitrogen incorporation.

(ii) The hopping conduction in an undoped CVD a-Si film disappears by the post-hydrogenation above room temperature.

(iii) The $\eta\mu\tau$ product of photoexcited excess carriers is increased by the post-hydrogenation. The nitrogen incorporation could increase the $\eta\mu\tau$ product of post-hydrogenated films.

REFERENCES

1) J.J. Hauser, Solid State Commun., 19 (1976) 1049.
2) A.K. Malhotra and G.W. Neudeck, Appl. Phys. Lett., 28 (1976) 47.
3) T. Tiedje, T.D. Moustakas, and J.M. Cebulka, Phys. Rev., B23 (1981) 5643.
4) T.D. Moustakas, Solar Energy Materials, 8 (1982) 187.
5) P. Viktrovitch, G. Moddel, J. Blake, S. Oguz, R.L. Weisfield, and W. Paul, J. de Physique, 42 (1982) C4-455.
6) W. Paul, A.J. Lewix, G.A.N. Connel, and T.D. Moustakas, Solid State Commun., 20 (1976) 969.
7) W. Paul and D.A. Anderson, Solar Energy Materials, 5 (1981) 229.
8) A.K. Ghosh, T. McMahon, E. Rock, and H. Wiesman, J. Appl. Phys., 50 (1979) 3407.
9) F.H. Cocks, A.J. Scharman, P.L. Jones, and S.F. Cogap, Appl. Phys. Lett., 36 (1980) 909.
10) B.A. Scott, P.M. Plecenic, and E.E. Simonyi, Appl. Phys. Lett., 39 (1981) 73.
11) B.S. Meyerson, B.A. Scott, and D.J. Wolford, J. Appl. Phys., 54 (1983) 1461.
12) S.C. Gau, B.R. Weinberger, M. Akhtar, Z. Kiss, and A.G. MacDiarmid, Appl. Phys. Lett., 39 (1981) 436.
13) M. Akhtar, V.L. Dolal, K.R. Ramaprasad, S. Gau, and A.J. Cambridge, Appl. Phys. Lett., 41 (1982) 1146.
14) I. Yamada, I. Nagai, M. Horie, and T. Takagi, J. Appl. Phys., 54 (1983) 1583.
15) M. Kobayashi, J. Saraie, and H. Matsunami, Appl. Phys. Lett., 41 (1981) 696.

16) P.G. LeComber, R.J. Loveland, W.E. Spear, and R.A. Vanghan, *Proc. 5th Int. Conf. on Amorphous & Liquid Semiconductors, Garmisch-Partenkirchen, 1973* (Taylor and Francis, London, 1974) p.245.

17) J. Magarino, D. Kaplan, A. Friederich, and A. Deneuville, Philos. Mag., B45 (1982) 285.

18) J.I. Pankove, Appl. Phys. Lett., 32 (1978) 812.

19) D. Kaplan, N. Sol, G. Velasco, and P.A. Thomas, Appl. Phys. Lett., 33 (1978) 285.

20) N. Sol, D. Kaplan, D. Dienmegard, and D. Durbreuil, J. Non-Cryst. Solids, 35-36 (1980) 291.

21) S. Hasegawa, D. Ando, Y. Kurata, and T. Shimizu, Philos. Mag., B47 (1983) 139.

22) P. Hey and B.O. Seraphin, Solar Energy Materials, 8 (1982) 215.

23) H. Kurata, M. Hirose, and Y. Osaka, Jpn. J. Appl. Phys., 20 (1981) L811.

24) J. Baixeras, D. Mancaraglia, and P. Andro, Philos. Mag., B37 (1978) 403.

25) R.W. Griffith, E.J. Kampas, P.E. Vanier, and M.D. Hirsh, J. Non-Cryst. Solids, 35-36 (1980) 391.

26) S.M. Pietruszco, K.L. Narasiman, and S. Guha, Philos. Mag., B43 (1981) 357.

27) H. Watanabe, K. Katoh, and M. Yasui, Jpn. J. Appl. Phys., 21 (1982) L341.

28) W.E. Spear and P.G. LeComber, Philos. Mag., 33 (1976) 935.

29) D.A. Anderson and W.E. Spear, Philos. Mag., 36 (1977) 695.

30) T. Saitoh, S. Muramatsu, T. Shimada, and M. Migitaka, Appl. Phys. Lett., 42 (1983) 678.

31) *The optical gap of films is 1.5 eV and 1.6 eV, respectively.*

IX. GLOW-DISCHARGE DEPOSITION OF AMORPHOUS SILICON-NITROGEN-HYDROGEN ALLOYS

9.1 INTRODUCTION

The glow-discharge (GD) deposition of SiN insulator and amorphous Si (a-Si) films was reported by *Sterling and Swann* in 1965.[1] Successively, several authors[2-4] reported properties of GD SiN films for passivation or gate insulator films. On the other hand, GD a-Si was interested as photoconductive thin films.[5] Although it had been supposed that the electrically active doping into a-Si was difficult,[5] the electrically active doping into GD a-Si was reported[6,7] by *Spear and LeComber* in 1975. In 1976, the a-Si solar cell[8-10] was fabricated from GD a-Si films. It was found that GD SiN insulator and a-Si films contain many hydrogen atoms bonded to silicon or nitrogen atoms up to 50 at.%.[4,11-14] Thus, these films are considered to be silicon-nitrogen-hydrogen (Si:N:H) or silicon-hydrogen (Si:H) alloys. Most of a-Si thin film devices have been fabricated from GD a-Si:H films so far. It seems that GD a-Si:H films have advantages to a-Si:H films prepared by other methods with respect to their applications to electrical devices at this stage.

In this chapter, preparation and fundamental properties of GD a-Si:N:H films are described. Here, these films are interested as active semiconductor films rather than passive insulator films.[15-17] Optical and electrical properties of these films are described in Chapter X.

9.2 PREPARATION

Amorphous Si:N:H alloys were deposited by rf (13.56 MHz) glow discharge of SiH_4, N_2, and H_2 gas mixture in a capacitive coupling reactor[18,19] in which the spacing and diameter of the electrodes are 2 cm and 20 cm, respectively. The rf excitation power was 40 W. Substrates were set on the anode. The substrate temperature was 250°C or 350°C. The total gas flow of N_2 and H_2 was maintained at 100 sccm,

and SiH_4 gas flow was 10 or 20 sccm. The total gas pressure was 1 Torr.

9.3 DEPOSITION RATE

It has been considered with respect to the deposition process of GD a-Si:H from SiH_4 that the SiH_4 molecules are dessociated into SiH_x ($x = 0, 1, 2,$ or 3) species by discharge, which are transported to the substrate surface and react at the surface.[20] It could be considered in an asymmetric capacitive coupling rf reactor that SiH_4 molecules are primely dissociated in the cathode sheath by collisions of electrons and the deposition onto substrates on the anode is dominated by the surface reaction of neutral species.[20]

Figure 9.1 shows the deposition rate of GD a-Si:N:H films at various gas flow rates and substrate temperature of 250°C. The deposition rate increases with the SiH_4 and N_2 gas flow rates. It is noted that the deposition rate at the N_2 gas flow rate of 100 sccm is remarkably higher than that at the N_2 gas flow rate below 80 sccm. It might be considered that the N_2 introduction into the reactant gas increases the electron concentration in the plasma, which enhances the dissociation of SiH_4 molecules.

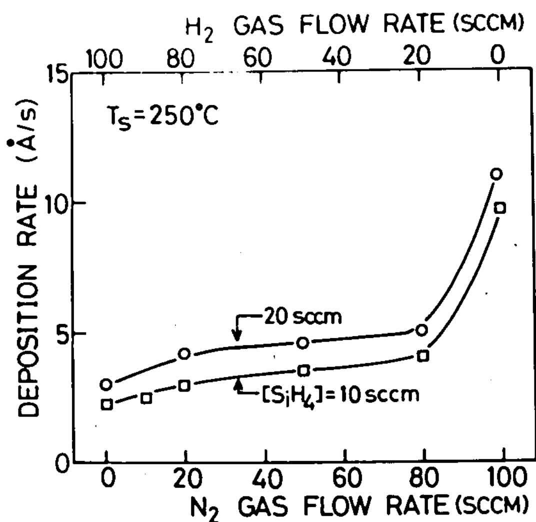

FIGURE 9.1 Deposition rate of GD a-Si:N:H films.

9.4 INFRARED ABSORPTION — NITROGEN AND HYDROGEN CONTENTS

The infrared transmittance spectra of 0.6 to 2-μm-thick GD a-Si:N:H films on crystalline Si substrates showed absorption around 820 cm^{-1} and 2000 cm^{-1}. It is considered that the former originates from Si-N bond vibrations and the latter from Si-H vibrations[4]. Absorption due to N-H bond vibrations around 1200 cm^{-1} or 3350 cm^{-1} was not detected. The incorporated nitrogen content in films was evaluated from the integrated absorption coefficient around 820 cm^{-1} as described in Chapter III. The nitrogen content in films prepared at various deposition conditions is shown in Fig.9.2. The nitrogen content increases with the N_2 gas flow rate and is saturated at the N_2 gas flow rate exceeding 50 sccm. The saturation of the nitrogen content would be associated with increases of the deposition rate of films with the N_2 gas flow rate as shown in Fig.9.1. The nitrogen content is increased by decreases of the SiH_4 gas flow rate and little influenced by the substrate temperatures of 250°C and 350°C. Thus, it is considered that the nitrogen content in films is primely related to the concentrations of active species in the plasma.

Figure 9.3 shows the peak wavenumber of Si-H absorption band of GD a-Si:N:H films, which are increased by the nitrogen incorporation.

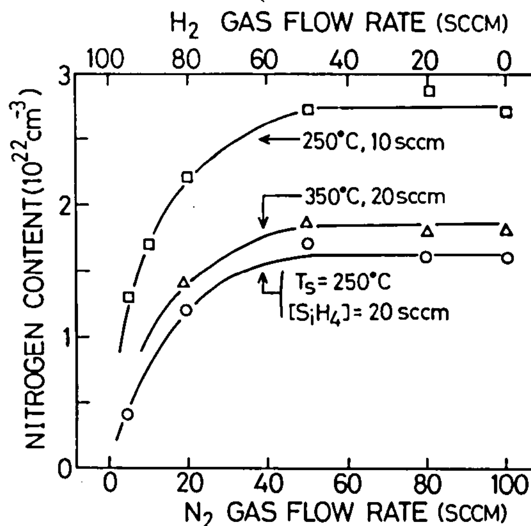

FIGURE 9.2 Nitrogen content of GD a-Si:N:H films.

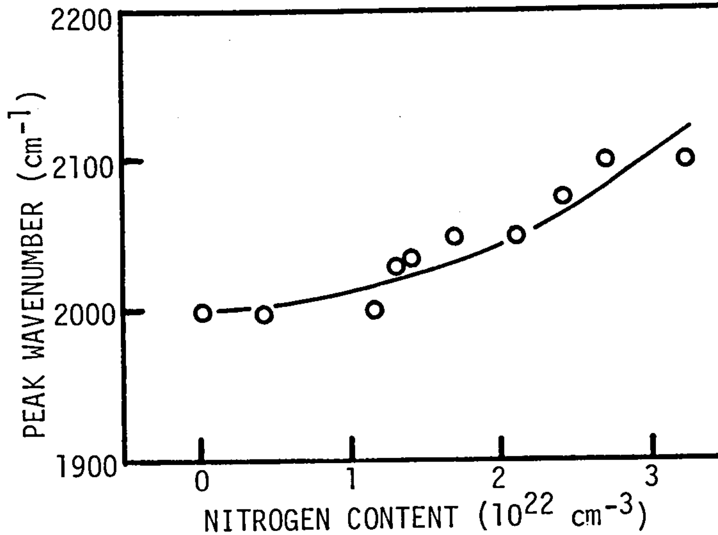

FIGURE 9.3 Peak absorption wavenumber of Si-H bond vibrations in GD a-Si:N:H films.

Since the peak wavenumber of undoped a-Si:H films is 2000 cm^{-1}, it is considered that the hydrogen atoms in the films are incorporated in the configurations of (SiH)≡3Si. The increase of the peak wavenumber by the nitrogen incorporation could be understood by increases in the electronegativity sum of neighbor atoms of Si-H oscillators due to the nitrogen incorporation.[21]

The relation between the incorporated hydrogen content and the infrared absorption coefficient has been reported on a-Si:H[22] and a-Si:N:H[23] films in which the mole fraction of Si/N is 0.7 to 1.4, and the proportion constant between them has been determined with respect to a-Si:H and a-Si:N:H films. Figure 9.4 shows the hydrogen content of GD a-Si:N:H films evaluated from the infrared absorption coefficient by utilizing the proportion constant on a-Si:H films.[22] However, when the proportion constant on a-Si:N:H films[23] was applied, the evaluated hydrogen content became larger by a factor of two. If the disagreement in the proportion constant resulted from the nitrogen incorporation into a-Si:H films, the hydrogen content of films containing more nitrogen atoms would be larger than the values shown

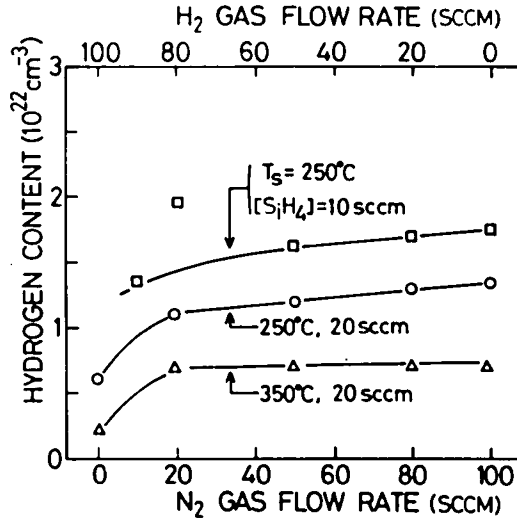

FIGURE 9.4 Hydrogen content of GD a-Si:N:H films evaluated by the infrared absorption.

in the figure. As shown in the figure, the films containing more nitrogen atoms tend to contain more hydrogen atoms at the substrate temperature of 250°C. Further, films deposited at 350°C and the N_2 gas flow rate of 20 sccm contain the comparable amount of hydrogen atoms with that in films at 250°C and 0 sccm. Therefore, it could be considered that the nitrogen incorporation into a film retains the hydrogen effusion from the solid phase during the deposition.

9.5 SUMMARY

Preparation of a-Si:N:H films by glow discharge of SiH_4, N_2, and H_2 gases has been described. The deposition rate and infrared transmittance spectra of films have been measured and discussed. The infrared absorption due to Si-N and Si-H bond vibrations was detected by infrared transmittance measurements. The nitrogen and hydrogen contents in films could be evaluated from their infrared transmittance spectra. Their results can be summarized as follows.

(i) The deposition rate is increased up to five times larger by the N_2 gas introduction into the reactant gas.

(ii) The nitrogen content is increased by the N_2 gas introduction into the reactant gas and saturated at the N_2 gas flow rate exceeding 50 sccm under the constant total gas flow of N_2 and H_2 of 100 sccm. Increases in the SiH_4 gas flow rate decrease the nitrogen content. The nitrogen content is little influenced by the substrate temperature of 250°C and 350°C.

(iii) The hydrogen content is increased with the H_2 gas flow rate, whereas decreased with the SiH_4 gas flow rate. Although the hydrogen content is decreased by the substrate temperature increase, the nitrogen incorporation suppresses the decrease of hydrogen contents caused by the substrate temperature increase.

REFERENCES

1) H.F. Sterling and R.C.G. Swann, Solid State Commun., 8 (1965) 653.
2) R.C.G. Swann, R.R. Mehta, and T.P. Cange, J. Electrochem. Soc., 114 (1967) 713.
3) Y. Kuwano, Jpn. J. Appl. Phys., 8 (1969) 876.
4) E.A. Taft, J. Electrochem. Soc., 118 (1971) 1341.
5) R.C. Chittick, J.H. Alexander, and H.F. Sterling, J. Electrochem. Soc., 116 (1969) 77.
6) W.E. Spear and P.G. LeComber, Solid State Commun., 17 (1975) 1193.
7) W.E. Spear and P.G. LeComber, Philos. Mag., 33 (1976) 935.
8) D.E. Carlson and C.R. Wronski, Appl. Phys. Lett., 28 (1976) 671.
9) D.E. Carlson, IEEE Trans. on Electron Devices, ED-24 (1977) 449.
10) Y. Hamakawa, Solar Energy Materials, 8 (1982) 101.
11) M.H. Brodsky, M. Cardona, and J.J. Cuomo, Phys. Rev., B16 (1977) 3556.
12) P.J. Zanucchi, C.R. Wronski, and D.E. Carlson, J. Appl. Phys., 48 (1977) 5227.
13) J.C. Knights, G. Lukovski, and R.J. Nemanich, Philos. Mag., B37 (1978) 467.

14) E.C. Freeman and W. Paul, Phys. Rev., B18 (1978) 4288.
15) D.A. Anderson and W.E. Spear, Philos. Mag., 35 (1977) 1.
16) H. Kurata, M. Hirose, and Y. Osaka, Jpn. J. Appl. Phys., 20 (1981) L811.
17) H. Watanabe, K. Katoh, and M. Yasui, Jpn. J. Appl. Phys., 21 (1982) L341.
18) J.C. Knights, Philos. Mag., 34 (1976) 663.
19) J.E. Potts, E.M. Peterson, and J.A. McMillan, J. Appl. Phys., 52 (1981) 6665.
20) M. Hirose and T. Hamasaki, Oyo Buturi, 52 (1983) 657 (*in Japanese*).
21) G. Lucovsky, Solid State Commun., 29 (1979) 571.
22) C.J. Fang, K.L. Gruntz, L. Ley, and M. Cardona, J. Non-Cryst. Solids, 35-36 (1980) 255.
23) W.A. Lanford and M.J. Rand, J. Appl. Phys., 49 (1978) 2473.

X. OPTICAL AND ELECTRICAL PROPERTIES OF GLOW-DISCHARGE DEPOSITED AMORPHOUS SILICON-NITROGEN-HYDROGEN ALLOYS

10.1 INTRODUCTION

The glow-discharge (GD) deposited amorphous silicon-hydrogen (a-Si:H) films applied to electrical devices usually contain about 10 at.% of the hydrogen atoms. These hydrogen atoms could not only decrease the defects but also increase the optical gap.[1-3] It has been supposed that decreasing of defects by hydrogenation is due to the termination of dangling bonds or the relaxation of average coordination number.

In previous chapters, properties of chemically vapor-deposited (CVD) a-Si:N alloys have been described, and effects of nitrogen incorporation on their properties have been discussed. These films could be considered to be binary alloys containing electrically active additives of hydrogen. On the other hand, GD a-Si:N:H films are considered to be ternary alloys. In this chapter, optical and electrical properties of GD a-Si:N:H ternary alloy films are described and discussed.

10.2 OPTICAL GAP

The optical gap of films derived from the $\sqrt{\alpha h\nu} - h\nu$ plot is shown in Fig.10.1. The optical gap is increased by the N_2 gas introduction into the reactant gas. As described in Chapter IX, the films deposited at the SiH_4 gas flow rate of 10 sccm and 250°C contain more nitrogen and hydrogen atoms than the films at 20 sccm at a fixed N_2 gas flow rate. Thus, these films have the wider optical gap than the films at the SiH_4 gas flow rate of 20 sccm. In films deposited at the SiH_4 gas flow rate of 20 sccm, the nitrogen content is almost independent of the substrate temperatures of 250°C and 350°C, whereas the hydrogen content of films at 250°C is larger than that of films at 350°C as described in Chapter IX. Such increases in the hydrogen content would yield the wider optical gap of films at 250°C than that

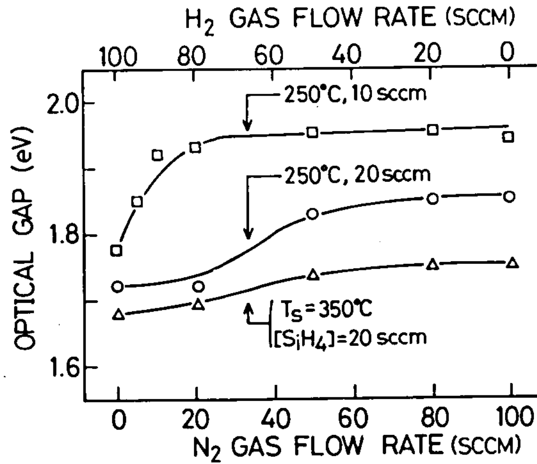

FIGURE 10.1 Dependence of optical gap of a-Si:N:H films on deposition conditions.

of films at 350°C.

10.3 DARK CONDUCTIVITY

Figure 10.2 shows the dark conductivity of films at room temperature, the activation energy, and the preexponential factor in the temperature dependence of the dark conductivity. A little incorporation of nitrogen atoms into films increases the dark conductivity, and further incorporation decreases it. It is noted that the films deposited at the SiH_4 gas flow rate of 10 sccm contain more nitrogen atoms than the films at 20 sccm. From the results shown in Fig.10.2, the increase in the dark conductivity by a little incorporation of nitrogen atoms is related to the decrease in the activation energy, which suggests an introduction of donors by the nitrogen incorporation.[4] On the other hand, the reduction in the dark conductivity could be due to the increase in the activation energy or the decrease of the preexponential factor. It could be considered that the increase in the activation energy results from the increase in the mobility gap, and the decrease of the preexponential factor results from the decrease of the mobility.

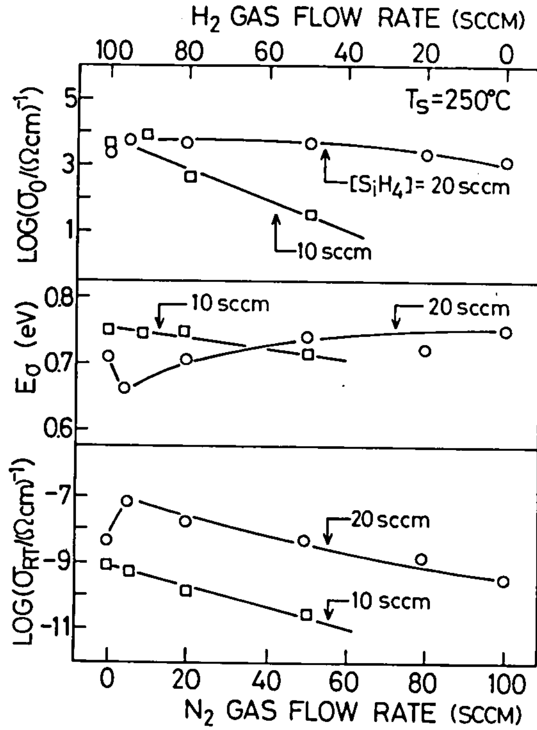

FIGURE 10.2 Dependence of preexponential factor, activation energy, and room temperature dark-conductivity of GD a-Si:N:H films on deposition conditions.

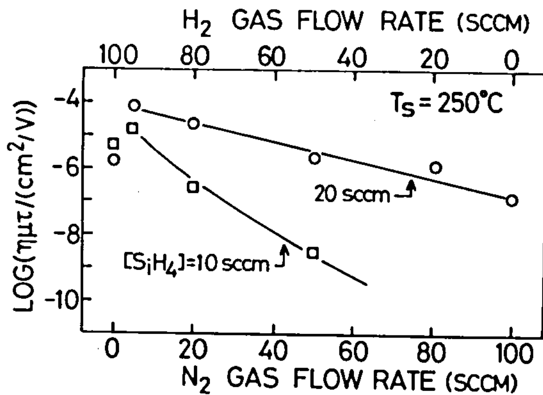

FIGURE 10.3 Dependence of product of quantum efficiency, mobility, and lifetime of GD a-Si:N:H films on deposition conditions.

10.4 PHOTOCONDUCTIVITY — PRODUCT OF QUANTUM EFFICIENCY, MOBILITY, AND LIFETIME

Figure 10.3 shows the normalized photoconductivity of the $\eta\mu\tau$ product at the incident photon energy of 2 eV, which is drastically increased by a small amount of N_2 gas introduction and the further introduction decreases it. It is noted that electrical properties of films at SiH_4 gas flow rate of 20 sccm and N_2 gas flow rate exceeding 50 sccm depend on the N_2 gas flow rate, although the hydrogen and nitrogen contents in films are independent of it. The reason might be associated with variations of hydrogen configurations. It was proposed that the mobility of a-Si:H films could be decreased by closely gathered hydrogen atoms which can be identified by the broad component in nuclear magnetic resonance.[5] The relation between the $\eta\mu\tau$ product and the dark conductivity is shown in Fig.10.4. These results suggest that the nitrogen incorporation strongly influences the mobility. However, the results on the $\eta\mu\tau$ products can be interpreted by a variation of the lifetime which could be strongly influenced by the shallow trap of the tail states and the recombination center of the deep gap states. Further study on these states will clarify the influence of nitrogen incorporation on the electrical properties.

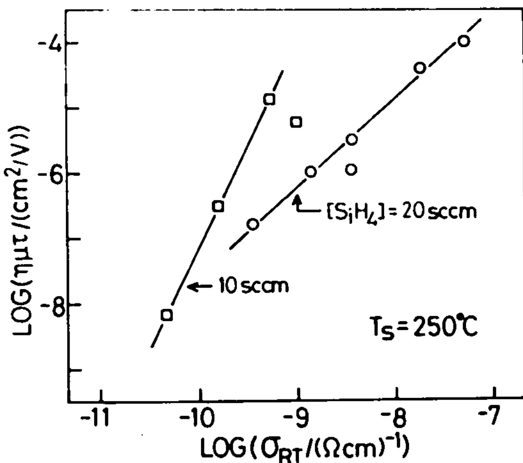

FIGURE 10.4
Relation between $\eta\mu\tau$ product and dark conductivity of GD a-Si:N:H films.

10.5 SUMMARY

Optical and electrical properties of GD a-Si:N:H films from SiH_4, N_2, and H_2 gases have been described and discussed. The results can be summarized as follows.

(i) The optical gap of films is increased by the N_2 gas introduction, the lowering of substrate temperature, and/or the decrease of the SiH_4 gas flow rate. Such variations of the optical gap could be understood in terms of the variation of incorporated nitrogen and hydrogen contents.

(ii) The dark conductivity is increased by a small amount of N_2 gas introduction, and further introduction decreases it.

(iii) The dependence of the photoconductivity of films on the SiH_4 and N_2 gas flow rates is similar to that of the dark conductivity. The strong correlation between the dark conductivity and the photoconductivity has been observed.

REFERENCES

1) J. Perrin, I. Solomon, B. Bourdon, J. Fontenille, and E. Liegeon, Thin Solid Films, 62 (1979) 327.
2) F.R. Jeffrey, H.R. Shanks, G.C. Danielson, J. Non-Cryst. Solids, 35-36 (1980) 261.
3) J.P. Deuville, T.D. Moustakas, A.F. Ruppert, and W.A. Lanford, J. Non-Cryst. Solids, 35-36 (1980) 481.
4) T. Noguchi, S. Usui, A. Sawada, Y. Kanoh, and M. Kikuchi, Jpn. J. Appl. Phys., 21 (1982) L485.
5) T. Shimizu, N. Nakazawa, M. Kumeda, and S. Ueda, Jpn. J. Appl. Phys., 21 (1982) 351.

XI. CONCLUSIONS

In this study, optical and electrical properties of amorphous silicon-nitrogen (a-Si:N) and amorphous silicon-nitrogen-hydrogen (a-Si:N:H) alloys have been systematically characterized and discussed. Amorphous Si:N binary alloy films were deposited by chemical vapor deposition (CVD) of SiH_4 and NH_3 gases in Ar, while a-Si:N:H ternary alloy films by glow-discharge decomposition of SiH_4, N_2, and H_2 gases. New characterization methods have been proposed and used to determine the gap-state density near the Fermi level and properties of trap states in metal/insulator/semiconductor (MIS) structures. Moreover, some ambiguous procedure in an analysis of the field-effect method has been taken off. The dependence of optical and electrical properties of binary CVD a-Si:N films and ternary GD a-Si:N:H films on deposition conditions, thermal annealing, or post-hydrogenation has been obtained. Further, the influence of the nitrogen incorporation into a-Si or a-Si:H films on the properties, defects, and gap states has been revealed.

In Chapter II, the gap-state density measurements reported in the previous literature have been reviewed and discussed. It has been concluded that the reported methods are insufficient to measurements of gap-state density of CVD a-Si and its alloy. Thus, a new method which would be called as the high-frequency capacitance-voltage method has been proposed to evaluate the gap-state density of CVD a-Si. It has been demonstrated that the method is useful for determination of the gap-state density near the Fermi level. Although it has been considered that there is the intrinsic ambiguity in the principle of the field-effect method, *e.g.*, influence of the interface states, it has been improved into the reliable method by solving rigorously the Poisson equation in the analysis. It has been obtained by means of these methods that the gap-state density of CVD a-Si deposited at 550°C is the order of 10^{17} $cm^{-3}eV^{-1}$ around the Fermi level and rapidly increases away from the Fermi level. The

gap-state density reaches the order of 10^{20} $cm^{-3}eV^{-1}$ at 0.4 eV below and above the Fermi level, provided the interface states are negligibly fewer than the bulk gap states.

The response time, capture cross section, and density of traps in MIS structures where the semiconductor is GD a-Si:H or CVD a-Si:N films have been evaluated by a new method from the frequency and temperature dependence of the flat-band capacitance. The response time of slow states was found to be $2.5\times10^{-11}\exp(0.72\text{eV}/k_BT)$ s in a GD a-Si:H MIS diode and $2.4\times10^{-9}\exp(0.6\text{eV}/k_BT)$ s in a CVD a-Si:N MIS diode. The trap densities were found to be about 10^{16} $cm^{-3}eV^{-1}$ for bulk traps and the order of 10^{11} $cm^{-2}eV^{-1}$ for interface traps in a GD a-Si:H MIS diode, while the order of 10^{18} to 10^{19} $cm^{-3}eV^{-1}$ for bulk traps and the order of 10^{12} to 10^{13} $cm^{-2}eV^{-1}$ for interface traps in a CVD a-Si:N MIS diode. The capture cross sections of traps in GD a-Si:H and CVD a-Si:N MIS diodes were found to be about 10^{-15} and 10^{-17} cm^2, respectively.

In Chapter III, preparation of a-Si:N alloys by chemical vapor deposition from SiH_4, NH_3, and Ar gases at 550°C has been described. It was found that the deposition rate is decreased by high NH_3 gas concentrations. The nitrogen content of films could be determined by their infrared absorptions, and that dependence on SiH_4 and NH_3 gas concentrations has been obtained. It has been suggested that the deposition of films is rate-limited by the gas phase decomposition at low NH_3 gas concentrations and the hydrogen desorption at high NH_3 gas concentrations. It has been also suggested that the heterogeneous reaction of NH_3 molecules limits the nitrogen incorporation rate.

In Chapter IV, the optical absorption and refractive index of CVD a-Si:N films have been presented. The optical gap is increased from 1.5 to 2.0 eV with 2.8×10^{22} cm^{-3} of the nitrogen incorporation. The dependence of the optical gap and refractive index of films on the nitrogen content has been quantatively examined. The dependence of the optical gap on the mole fraction of nitrogen atoms to silicon

atoms, x, could be represented by $E_{opt} = 1.5 + 3.5(3x/4)^2$ eV .
The dependence of the refractive index on the nitrogen content has been also obtained.

In Chapter V, the influence of the nitrogen incorporation on dark conductivity and photoconductivity of CVD a-Si films has been investigated. The hopping conduction is drastically reduced by the nitrogen incorporation, whereas the extended-states conduction or photoconductivity is little influenced. The results on hopping conduction could be understood by the reduction of the gap-state density due to the nitrogen incorporation.

In Chapter VI, the influence of the nitrogen incorporation on defects and gap states in CVD a-Si has been examined by means of electron spin resonance (ESR) and field-effect measurements. It has been observed that the number of paramagnetic defects and the field-effect gap-state density at $E_F + 0.1$ eV $< E < E_F + 0.2$ eV are decreased to one-fifth by the nitrogen incorporation at which the mole fraction of nitrogen atoms to silicon atoms is 0.2. However, the field-effect gap-state density above $E_F + 0.3$ eV is increased by it. Further, the field effect of films was changed from an intrinsic to n-type characteristic by the nitrogen incorporation, which suggests donor introduction with the nitrogen incorporation.

In Chapter VII, the origin of such reductions of defects and gap states has been investigated by means of thermal annealing. Both the number of paramagnetic defects and the field-effect gap-state density in CVD a-$SiN_{0.2}$ films are increased by thermal annealing, which suggests that a small amount of hydrogen atoms can be contained in films. The hopping conduction is also increased by thermal annealing, which agrees with results on paramagnetic defects and the field-effect gap-state density. However, it seems that the reduction of defects and gap states by the nitrogen incorporation is due to the reduction of internal strain without creation of the dangling bonds, since the number of paramagnetic defects in thermally annealed film is decreased by the nitrogen incorporation.

In Chapter VIII, effects of post-hydrogenation of CVD a-Si:N films on their electrical properties have been investigated. It has been obtained that the nitrogen incorporation introduces donors into CVD a-Si films and increases the photoconductivity of post-hydrogenated films.

In Chapter IX, preparation of a-Si:N:H alloys by glow-discharge deposition from SiH_4, N_2, and H_2 gases has been described. It was found that the N_2 gas introduction increases the deposition rate. The nitrogen and hydrogen contents in films have been evaluated by the infrared absorptions. It has been shown that the nitrogen incorporation increases the hydrogen content.

In Chapter X, the optical and electrical properties of GD a-Si:N:H films have been presented. The optical gap is increased by the N_2 gas introduction, the lowering of substrate temperature, and/or the decrease of the SiH_4 gas flow rate. The variation could be understood in terms of variations of incorporated nitrogen and hydrogen contents. The dark conductivity and photoconductivity are increased by a small amount of N_2 gas introduction and decreased by the further introduction. The strong correlation between the dark conductivity and photoconductivity has been found.

It could be suggested that further investigations on structures, transport properties, recombination or trapping mechanism, and shallow states are required for detailed understandings of properties of a-Si:N or a-Si:N:H alloys and further applications of them to electrical devices.

APPENDIX

A. ENERGY BAND DIAGRAM OF AMORPHOUS Si/CRYSTALLINE Si JUNCTIONS

Figure A.1 shows the possible energy band diagrams of CVD a-Si/ n-type crystalline Si (c-Si) junctions which are classified by the electron affinity of CVD a-Si, χ_a (eV). A differential capacitance of the c-Si space charge region is calculated for each case in the figure.

Taking accumlated free carriers into account, the differential capacitance of the c-Si space charge region, $C_{c(\psi_c)}$, where ψ_c is a voltage across the space charge region, can be calculated by the same manner to the evaluation in MIS diodes (*see example*, S.M. Sze, *Physics of Semiconductor Devices*, *2nd ed.*, John Wiley & Sons, New

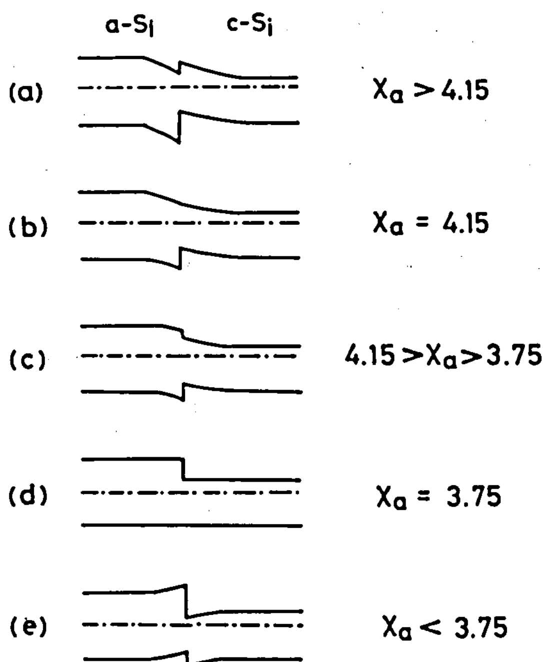

FIGURE A.1 Possible energy band diagrams of CVD a-Si/n-type c-Si junctions which are classified by the electron affinity of CVD a-Si, χ_a (eV).

York, 1981, Chapter 7) for $\psi_c \geqq 0$ as

$$C_{c(\psi_c)} = \frac{\varepsilon_c \varepsilon_0 |\exp(\beta\psi_c) - 1 + (n_i/n_B)^2[1 - \exp(-\beta\psi_c)]|}{L_D F_{(\psi_c)}} \quad , \tag{A.1}$$

where

$$\beta = q/k_B T \ , \quad L_D = \sqrt{2k_B T \varepsilon_c \varepsilon_0 / n_B q^2} \ ,$$

$$F_{(\psi_c)} = \{\exp(\beta\psi_c) - \beta\psi_c - 1 + (n_i/n_B)^2[\exp(-\beta\psi_c) + \beta\psi_c - 1]\}^{1/2} \ ,$$

and n_B and n_i are the free electron concentrations of n-type and intrinsic c-Si. Here, the condition of $\psi_c \geqq 0$ is satisfied in the cases (d) and (e). For the cases (a) to (c), ψ_c is negative, at which it can be easily shown by the analogy to the MIS diode that $C_{c(\psi_c)} < C_{c(0)}$ for high frequencies to which the generation of holes in an n-type c-Si cannot respond. It is noted that for $\psi_c > 0$ the capacitance $C_{c(\psi_c)} > C_{c(0)}$ from Eq.(A.1).

As described in Chapter II, the total differential capacitance C is given by the series of those of the CVD a-Si film and c-Si space charge region. Thus, we can obtain the total capacitance with respect to each case shown in Fig.A.1. Figure A.2 shows a typical C-V characteristic of 2000-Å-thick CVD a-Si/n-type c-Si ($n_B = 2 \times 10^{15}$ cm^{-3}) at room temperature and 1 MHz for which the CVD a-Si is dielectric. The applied voltage is positive when the potential of a-Si is higher than c-Si, and *vice versa*. The high-frequency differential capacitance at $V = 0$ is about 4.8×10^{-8} Fcm^{-2}. On the other hand, the predicted capacitance for the cases (a) to (e) in Fig.A.1 is

$$\left.\begin{array}{ll} C \leqq 3.5 \times 10^{-8} \ (\mathrm{Fcm}^{-2}) & \text{for (a) to (d),} \\ \text{or} \quad 3.5 \times 10^{-8} < C < 5.2 \times 10^{-8} \ (\mathrm{Fcm}^{-2}) & \text{for (e).} \end{array}\right\} \tag{A.2}$$

Therefore, the energy band diagram of CVD a-Si/n-type c-Si junction at $V = 0$ could be represented by Fig.A.1(e).

It can be confirmed that the space charge region is formed by

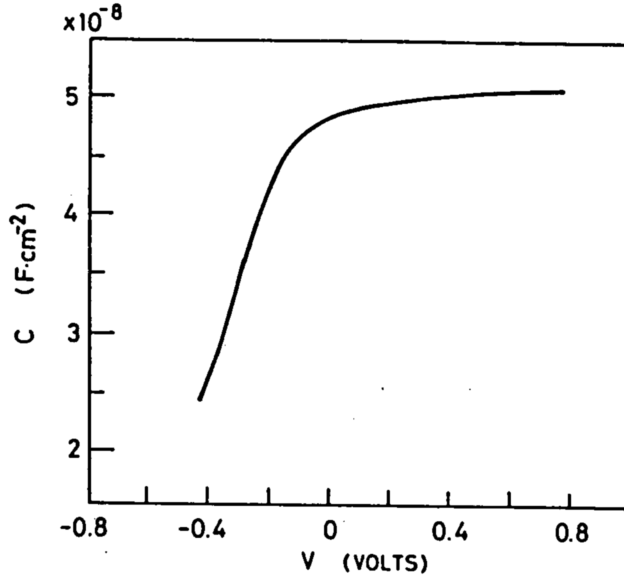

FIGURE A.2 A typical *C–V* characteristic of CVD a-Si/n-type c-Si ($n_B = 2 \times 10^{15}$ cm^{-3}) junctions in which the a-Si thickness is 2000 Å at 1 MHz.

charged gap states in CVD a-Si near CVD a-Si/n-type c-Si interface, and the space charge in CVD a-Si, Q_a, is equal to $-Q_c$ where Q_c is the total space charge in c-Si. Figure A.3 shows the effective interface charge evaluated from the *C–V* characteristic shown in Fig. A.2 , where the effective interface charge is a converted value of space charges in a-Si weighed with x/d = distance of space charges from metal-a-Si interface/CVD a-Si thidkness (*see*, E.H. Snow *et al*, J. Appl. Phys., 36 (1965) 1664). If the space charges in a-Si locate just at the CVD a-Si/c-Si interface, the effective interface charge is equal to the space charge density in a-Si. In the figure, the calculated space charge density in c-Si, Q_c, is also shown. Here, Q_c can be represented by

$$Q_c = -\frac{\psi_c 2k_B T \varepsilon_c \varepsilon_0}{|\psi_c| q L_D} F(\psi_c) \quad , \tag{A.3}$$

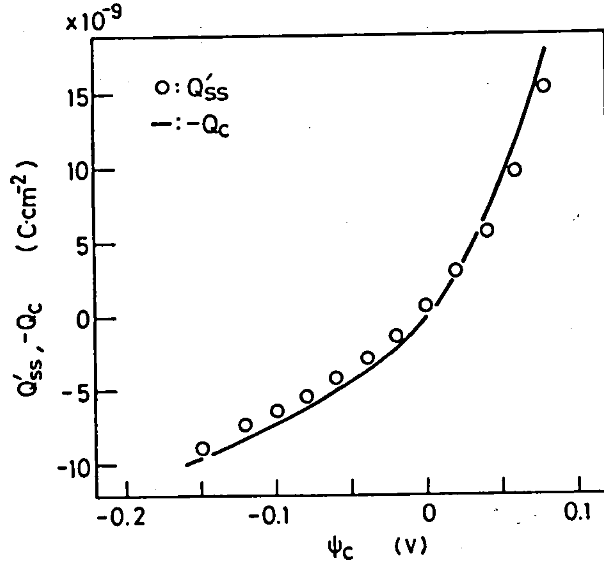

FIGURE A.3 Effective interface charge Q'_{ss} in CVD a-Si film and the space charge density in n-type c-Si, Q_c.

from the analysis of the space charge region in an MIS diode (*see*, S.M. Sze, *Physics of Semiconductor Devices, 2nd ed.*, John Wiley & Sons, New York, 1981, Chapter 7). As shown in Fig.A.3, the effective interface charge in metal/CVD a-Si/n-type c-Si structure agrees well with $-Q_c$. Therefore, it is considered that the space charge in a-Si locates near the a-Si/c-Si interface and that amount is equal to $-Q_c$ for a voltage application to CVD a-Si/n-type c-Si junctions.

The gap-state density is derived from the relationship of ψ_a and Q_a by the following expression:

$$N(E_F + q\psi_a) = \frac{1}{q\varepsilon_a\varepsilon_0}\frac{d}{d(q\psi_a)}\left(Q_a\frac{dQ_a}{d\psi_a}\right) , \tag{A.4}$$

which can be derived from the equations described by M. Hirose, T. Suzuki, and D.H. Doehler in Jpn. J. Appl. Phys., 18 (1979) suppl. 18-1, 109.

B. DETAILED DESCRIPTION ON FREQUENCY AND TEMPERATURE DEPENDENCE OF a-Si MIS DIODE FLAT-BAND CAPACITANCE

Based on the equivalent circuit shown in Fig.2.8, the capacitance C could be represented by

$$C = \frac{C_i\{(C_1+C_2)(C_i+C_1+C_2)+\omega^2[\tau_1^2(C_iC_2+C_2^2)+\tau_2^2(C_iC_1+C_1^2)+2\tau_1\tau_2C_1C_2]\}}{(C_i+C_1+C_2)^2+\omega^2[\tau_1^2(C_i+C_2)^2+\tau_2^2(C_i+C_1)^2+2\tau_1\tau_2C_1C_2]+\omega^4\tau_1^2\tau_2^2C_i^2}, \quad \text{(A.5)}$$

where $\tau_1 = C_1R_1$, $\tau_2 = C_2R_2$, and ω is the angular frequency. The frequency dependence of the capacitance at $\tau_1 \ll \tau_2$ is schematically shown in Fig.A.4. In the frequency range I, both the fast states having the response time of τ_1 and the slow states of τ_2 fully respond to the measurement signal. In the frequency ranges II and III, the fast states fully respond, whereas the slow states do not. In the frequency range IV, both the fast and slow states are hard to respond. In the frequency ranges I∿III, the capacitance is approximated by

$$\frac{C}{C_i} = \frac{C_1+C_2}{C_i+C_1+C_2}\left(\frac{1+a\omega^2\tau_2^2}{1+b\omega^2\tau_2^2}\right), \quad \text{(A.6)}$$

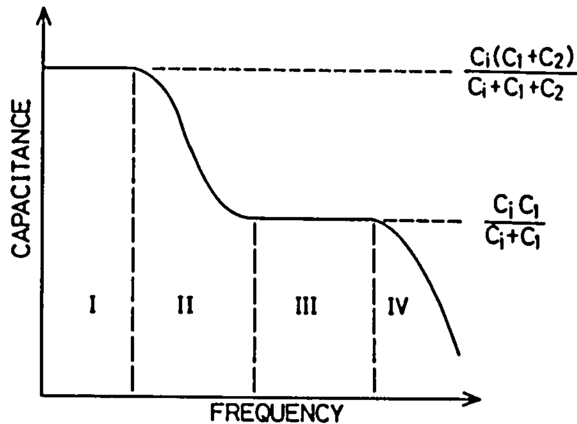

FIGURE A.4 Schematic illustration of frequency dependence of a-Si MIS diode capacitance with two response times of traps.

where

$$a = \frac{C_1(C_i + C_1)}{(C_1 + C_2)(C_i + C_1 + C_2)} ,$$

and

$$b = \left(\frac{C_i + C_1}{C_i + C_1 + C_2}\right)^2 .$$

If the response of traps can be approximated by one pair of C-R elements, we can obtain the frequency dependence represented by

$$C = \frac{C_s}{1 + (\omega C_s R_1)^2} , \quad \text{(A.7)}$$

where

$$C_s = \frac{C_i C_1}{C_i + C_1} .$$

In this case, the capacitance decreases monotonically with the frequency. However, the capacitance expressed by Eq.(A.7) is not consistent with the experimental results shown in Fig.2.7. Here, it is noted that increases in measurement temperature decrease the response time, which is equivalent to decreases in frequencies.

As shown in Fig.A.4, C_1 and C_2 can be determined from the capacitances which is little dependent on frequency in the regions I and III, since the insulator capacitance is obtained from the thickness and dielectric constant. In the experimental results shown in Fig.2.7, the variation of capacitance could be represented by Eq. (A.6) for those above 110°C. Thus, the response time of slow states at temperatures above 110°C could be obtained as shown in Fig.2.9.

The trap density is related to the capacitances in the equivalent circuit shown in Fig.2.8. If the traps originate from the a-Si bulk gap states, the trap densities of slow states and fast states, N_1 and N_2 can be evaluated from C_1 and C_2 by

$$C_1 = \left(\frac{q\varepsilon_a\varepsilon_0}{N_1 + N_2}\right)^{1/2} N_1 ,$$

and

$$C_2 = \left(\frac{q\varepsilon_a\varepsilon_0}{N_1 + N_2}\right)^{1/2} N_2 . \tag{A.8}$$

If the traps originate from the interface states, the trap density can be obtained from $C = qN$.

C. DERIVATION OF EQUATION (3.6)

Since the number of Si atoms is assumed to vary linearly with x and equal to 5×10^{22} cm^{-3} at $x = 0$ and 4×10^{22} cm^{-3} at $x = 4/3$ in SiN_x, the number of Si atoms, C_{Si} is varied with x as

$$C_{Si} = 5 \times 10^{22}(1 - 3x/4) + 4 \times 10^{22}(3x/4) \quad (\text{cm}^{-3}). \tag{A.9}$$

Since $x = C_N/C_{Si}$ by definition, one can obtain

$$10^{22}(3/4)x^2 - 5 \times 10^{22}x + C_N = 0 \quad . \tag{A.10}$$

The expression on x is easily obtained from Eq.(A.10).

D. DERIVATION OF EQUATION (3.9)

Since the decomposition of adsorbed NH_3 molecules is the rate-limiting, the nitrogen incorporation rate R_N equals $k_5[NH_3*]$. From definitions, $[NH_3*] = K_4[NH_3][*]$, and $[NH_3*] + [*] = N_s$, which yield

$$[NH_3*]\left(1 + \frac{1}{K_4[NH_3]}\right) = N_s \quad . \tag{A.11}$$

Thus, the expression on R_N is obtained.

ADDENDUM

Publications

Journal of Applied Physics (U.S.A.);

(1) *Gap-state measurement of chemically vapor-deposited amorphous silicon: High-frequency capacitance-voltage method,*

Goro Sasaki, Shizuo Fujita, and Akio Sasaki,

vol.53, No.2, pp.1013-1017 (1982).

(2) *Defect states and donors in thermally annealed or post-hydrogenated chemically vapor-deposited amorphous SiN_x alloy,*

Goro Sasaki, Shizuo Fujita, and Akio Sasaki,

vol.54, No.5, pp.2696-2700 (1983).

(3) *Deep traps in metal-insulator-chemically vapor-deposited amorphous SiN_x diodes,*

Goro Sasaki, Shizuo Fujita, and Akio Sasaki,

vol.54, No.7, pp.4008-4013 (1983).

(4) *Frequency dependence of flat-band capacitance of metal/insulator/glow-discharge deposited hydrogenated amorphous silicon diodes,*

Goro Sasaki, Shizuo Fujita, and Akio Sasaki,

to be published (Communications).

Japanese Journal of Applied Physics (Japan);

(5) *Effects of nitrogen incorporation on gap-state density in chemically vapor-deposited amorphous silicon,*

Goro Sasaki, Makoto Kondo, Shizuo Fujita, and Akio Sasaki,

vol.21, No.6, pp.L377-L378 (1982) (Letters).

(6) *Properties of chemically vapor-deposited amorphous SiN_x alloys,*

Goro Sasaki, Makoto Kondo, Shizuo Fujita, and Akio Sasaki,

vol.21, No.10, pp.1394-1399 (1982).

Journal of Non-Crystalline Solids (Netherlands);

(7) *Measurements of localized-state density in chemically vapor deposited amorphous silicon by the field-effect method,*

Masayuki Fujita, Goro Sasaki, Shizuo Fujita, and Akio Sasaki,

vol.46, No.3, pp.235-246 (1981).

(8) *Preparation and properties of glow-discharge deposited amorphous Si:N:H alloys from* SiH_4, N_2, *and* H_2 *gases,*

Goro Sasaki, Toshiyuki Tanaka, Masaya Okamoto, Shizuo Fujita, and Akio Sasaki,

in press.

Solar Energy Materials (Netherlands);

(9) *Some problems in determination of gap-state density in amorphous silicon,*

Tadashi Sasaki, Goro Sasaki, and Akio Sasaki,

vol.8, Nos.1-3, pp.293-302 (1982).

Oral Presentations

International Conference:

(1) *Preparation and properties of glow-discharge deposited amorphous Si:N:H alloys from* SiH_4, N_2, *and* H_2 *gases,*

Goro Sasaki, Toshiyuki Tanaka, Masaya Okamoto, Shizuo Fujita, and Akio Sasaki,

The 10th International Conference on Amorphous and Liquid Semiconductors, Tokyo, August (1983),

The proceedings are published as (8) in *Publications*.

Domestic Meetings:

The Institute of Electronics and Communication Engineers of Japan;

(1) *Measurements of the density of deep electronic states in CVD a-Si by high-frequency C-V method,*

Goro Sasaki, Shizuo Fujita, and Akio Sasaki,

Trans. 1980 Joint Conv. of Elect. Insts. of Kansai Section, Osaka, November, 1980, S5-4.

(2) *Measurements and deposition-parameter dependence of electric properties of CVD a-Si,*

Goro Sasaki, Masayuki Fujita, Shizuo Fujita, and Akio Sasaki,

Rept. Tech. Group of Semiconductor and Semiconductor Devices, SSD80-117 (1980).

(3) *The density of deep localized states in CVD a-Si,*

Goro Sasaki, Masayuki Fujita, Shizuo Fujita, and Akio Sasaki,

1980 Nat. Conv. Rec. of Semiconductor and Material Div., Kanazawa, October, 1980, S5-4.

(4) *Deep gap-states in chemically vapor-deposited amorphous silicon—Dependence on silane gas concentration, annealing effect, and nitrogen doping,*

Goro Sasaki, Makoto Kondo, Shizuo Fujita, and Akio Sasaki,

Rept. Tech. Group of Semiconductor and Semiconductor Devices, SSD81-115 (1981).

(5) *The frequency dependence of the capacitance of an a-Si MIS diode and the effect of free carriers on the field-effect method,*

Goro Sasaki, Shizuo Fujita, and Akio Sasaki,

Rept. Tech. Group of Semiconductor and Semiconductor Devices, SSD82-174 (1982).

The Japan Society of Applied Physics;

(1) *Characteristics of MIS diodes using semi-insulating amorphous Si,*

Goro Sasaki, Shizuo Fujita, Keisuke Ishio, and Akio Sasaki,

Yamanashi Univ., April, 1980, 3p-T-5.

(2) *Measurement method of a-Si gap states by the high-frequency C-V characteristics,*

Goro Sasaki, Shizuo Fujita, and Akio Sasaki,

Nagoya Inst. of Technology, October, 1980, 17p-Y-4.

(3) *The dependence of electrical properties of CVD a-Si on preparation conditions,*

Goro Sasaki, Masayuki Fujita, Shizuo Fujita, and Akio Sasaki,

Hosei Univ., April, 1981, 1p-S-17.

(4) *Temperature dependence of the field effect in CVD a-Si,*
Goro Sasaki, Shizuo Fujita, and Akio Sasaki,
Fukui Univ., October, 1981, 8a-A-5.

(5) *Electrical properties of nitrogen doped CVD a-Si,*
Goro Sasaki, Makoto Kondo, Shizuo Fujita, and Akio Sasaki,
Science Univ. of Tokyo, April, 1982, 2p-Y-4.

(6) *Annealing effect on electrical properties of CVD a-SiN_x films,*
Goro Sasaki, Shizuo Fujita, and Akio Sasaki,
Kyushu Univ. of Industry, September, 1982, 30a-X-1.

(7) *Measurements of response time of slow states in CVD a-SiN_x MIS structures,*
Goro Sasaki, Shizuo Fujita, and Akio Sasaki,
Chiba Univ., April, 1983, 4a-A-3.

(8) *Electrical and optical properties of GD a-SiN_x:H films deposited from SiH_4, N_2, and H_2 gases,*
Masaya Okamoto, Toshiyuki Tanaka, Goro Sasaki, Shizuo Fujita, and Akio Sasaki,
Chiba Univ., April, 1983, 5a-B-5.